Bioorganic Chemistry 88 (2019) 102923

Contents lists available at ScienceDirect

Bioorganic Chemistry

journal homepage: www.elsevier.com/locate/bioorg

Synthesis, antitumor testing and molecular modeling study of some new 6-substituted amido, azo or thioureido-quinazolin-4(3*H*)-ones

Mohamed A. Sabry[a,*], Heba A. Ewida[b], Ghada S. Hassan[a], Mariam A. Ghaly[a], Hussein I. El-Subbagh[a,*]

[a] Department of Medicinal Chemistry, Faculty of Pharmacy, Mansoura University, P.O. Box 35516, Mansoura, Egypt
[b] Department of Pharmacology and Biochemistry, Faculty of Pharmaceutical Sciences & Pharmaceutical Industries, Future University in Egypt, 12311 Cairo, Egypt

ARTICLE INFO

Keywords:
Synthesis
Substituted-quinazolin-4(3*H*)-one
Antitumor testing
Cell viability assay
DHFR inhibition
Molecular modeling study

ABSTRACT

A new series of 6-substituted amido, azo or thioureido-quinazolin-4(3*H*)-one was synthesized and tested for their *in-vitro* antitumor activity. Compounds **21**, **53** and **60** showed broad spectrum antitumor activity with average IC_{50} values of 6.7, 7.6 and 9.1 μM, respectively compared with methotrexate (**1**, IC_{50} 19.26 μM). As an attempt to reveal the mechanism of the antitumor potency, cell cycle analysis and DHFR inhibition were performed. Compounds **59** and **61** induced their cytotoxicity in Hela (IC_{50} 10.6 μM) and HCT-116 (IC_{50} 15.5 μM) cell lines, respectively through Pre-G1 apoptosis, inhibiting cell growth at G2-M phase. Compounds **29**, **33**, **59** and **61** showed DHFR inhibitory potency at IC_{50} 0.2, 0.2, 0.3 and 0.3 μM, respectively. The active DHFR inhibitors showed high affinity binding toward the amino acid residues Thr56, Ser59 and Ser118. The active compounds obeyed Lipinski's rule of five and could be used as template model for further optimization.

1. Introduction

Quinazolines as anticancer agents have been in the focus since the discovery of raltitrexed (**1**) and thymitaq (**2**) as thymidylate synthetase (TS) inhibitors [1–3]. 6-Arylamino-7-chloro-quinazoline-5,8-dione derivatives (**3**) showed antineoplastic potency against human A549 lung, and SNU-638 stomach cancer cell lines [4–6]. Quinazolines inhibit EGFR (epidermal growth factor receptor) tyrosine kinase overexpression through the inhibition of EGFR autophosphorylation and EGF-stimulated signal transduction [7–9]. Quinazolines also exert their antitumor activity through inhibition of the DNA repair enzyme system [10–14]. The pteridine containing lead methotrexate (MTX, **4**), the quinazoline skeleton of trimetrexate (**5**) and its pyrido[2,3-*d*]pyrimidine bioisoster piritrexim (**6**) are dihydrofolate reductase (DHFR) inhibitors exhibited an essential role in clinical medicine as antitumor agents [15–17], Fig. 1.

The activity of DHFR is linked to TS which catalyzes the reductive methylation of dUMP to dTMP [18]. The inhibition of DHFR prevents the growth of cancer cells and depletes the cell from thymine causing thymineless death. Accordingly, DHFR inhibition becomes the target for new antitumor drugs [19]. This revealed the importance of quinazoline nucleus concerning its binding affinity toward DHFR. Different hydrophobic and hydrophilic interactions for quinazolines were observed with Phe31, phe34, Thr56, Ser59 and Lys55 amino acid residues in the DHFR active site [20,21].

Compounds containing thioether (**7**–**9**), amide (**10**), azo- (**11**) and thioureido- (**12**) functional groups known to enhance antitumor activity, Fig. 2 [22–26]. Combining the inherited antitumor and DHFR inhibition activity of quinazolines and the antitumor potency enhancer functional groups in one structure is anticipated to produce compounds with more antitumor and/or DHFR inhibition activities [20,21,27–30]. The designed hybrids and their structure features (**A**, **B**, and **C**), fitted with electron donating or withdrawing functional groups, illustrated in Fig. 2, were synthesized and evaluated for their antitumor activity. As an attempt to reveal the antitumor potency mode of action, cell cycle analysis was performed and DHFR inhibition activity was evaluated. Moreover, Conformational analysis, molecular docking, flexible alignment, surface mapping, ADMET-study and compliance to the Lipinski's rule of five were investigated. The present study, aim to synthesis new quinazoline analogues, hoping to reach potentiated antitumor with DHFR inhibitory activity.

2. Results and discussion

2.1. Chemistry

The designed compounds **A**, **B** and **C** were synthesized adopting the

* Corresponding authors.
E-mail addresses: mohamedas1992@yahoo.com (M.A. Sabry), subbagh@yahoo.com (H.I. El-Subbagh).

https://doi.org/10.1016/j.bioorg.2019.102923
Received 28 January 2019; Received in revised form 1 April 2019; Accepted 10 April 2019
Available online 10 April 2019

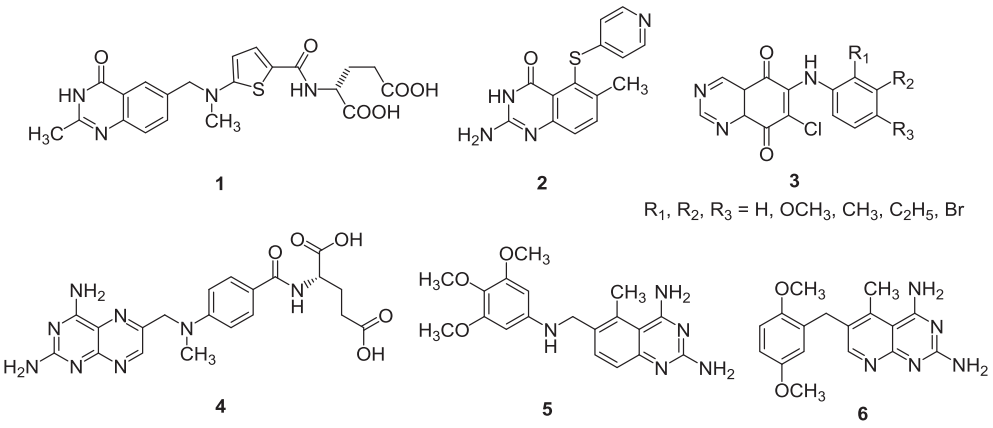

Fig. 1. Structures of some lead compounds.

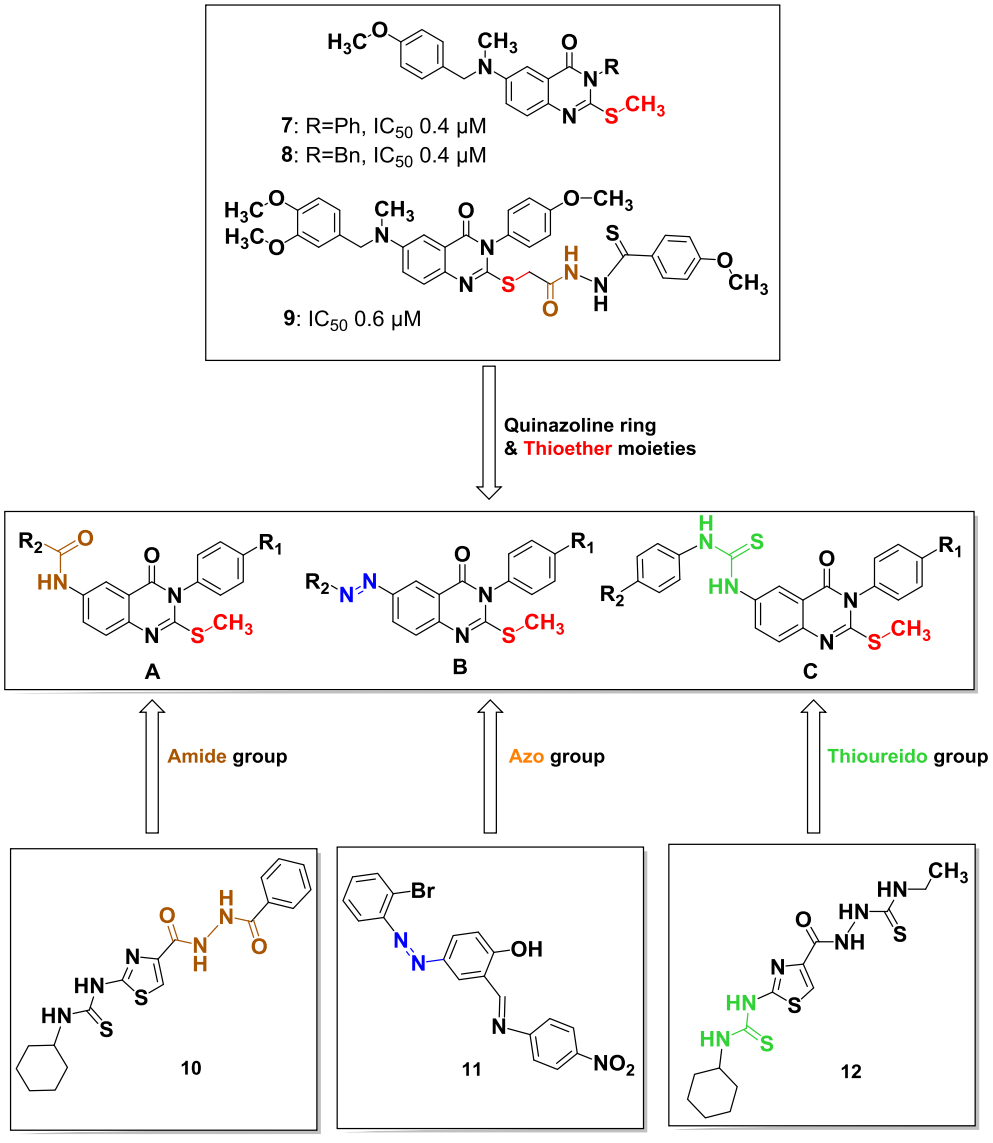

Fig. 2. Combining structure features of quinazoline, thioether, amide (A), azo (B) and thioureido (C) moieties.

routes outlined in Schemes 1–4. The starting materials 2-Mercapto-3-(4-substituted-phenyl)-6-substituted-quinazolin-4(3*H*)-ones (**16**, **17**) were obtained by reacting 5-nitro-anthranilic acid (**13**) and 4-substituted-phenyl isothiocyanates (**14** and **15**) using reported reaction conditions [21,29–31]. The 2-mercapto- functions of **16** and **17** was methylated using methyl iodide to produce **18** and **19**. Refluxing the 6-nitro-quinazolines **18** and **19** with stannous chloride in acetone gave the 6-amino analogues **20** and **21**, (Scheme 1, Table 1).

The 6-amino function of **20** and **21** was utilized to synthesize the amide derivatives **25–30**, **32**, **33** and **37–42** using variety of acid

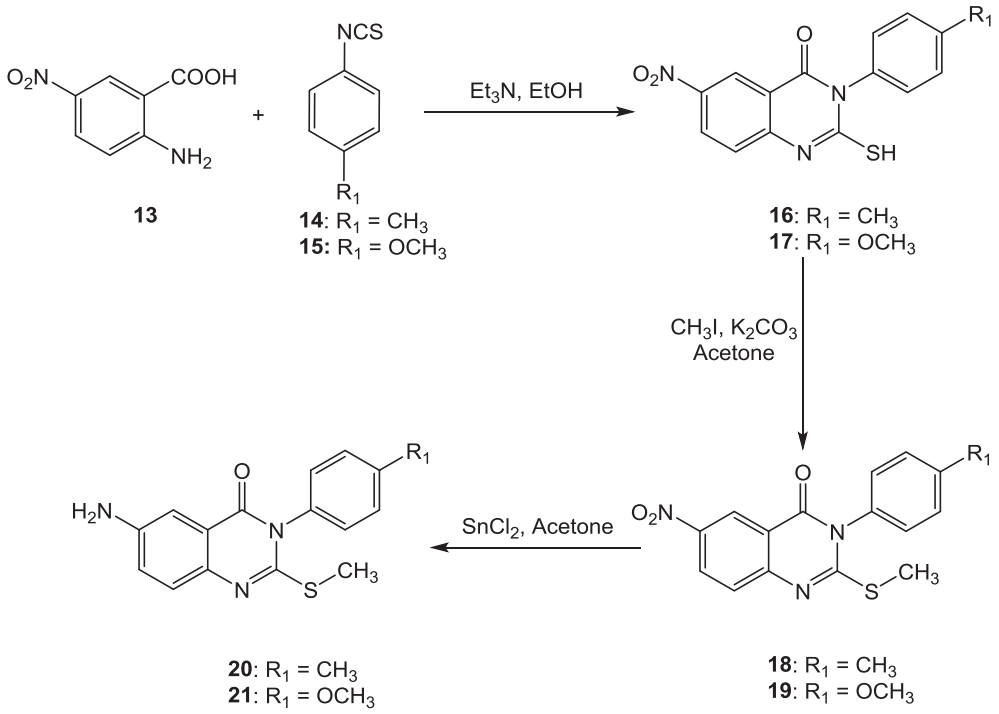

Scheme 1. Synthesis of the target compounds **16–21**.

chlorides (Scheme 2), the azo derivatives **45–48**, **50**, **51**, **53** and **54** using various phenolic coupling reagents (Scheme 3), and the thiourea analogues **56–61** upon treating with 4-substituted phenyl isothiocyanate derivatives (Scheme 4). Structure elucidation of the synthesized compounds was attained by the use of elemental analyses, in conjunction with MS, ^1H and ^{13}C NMR spectra.

2.2. Biological evaluation

2.2.1. Antitumor screening

The synthesized compounds **16–21**, **25–30**, **32**, **33**, **37–42**, **45–48**, **50**, **51**, **53**, **54** and **56–61** were evaluated for their antitumor activity *via* standard MTT assay [32–34], using four human tumor cell lines namely; HCT-116 colorectal carcinoma, MCF-7 breast, PC-3 prostate

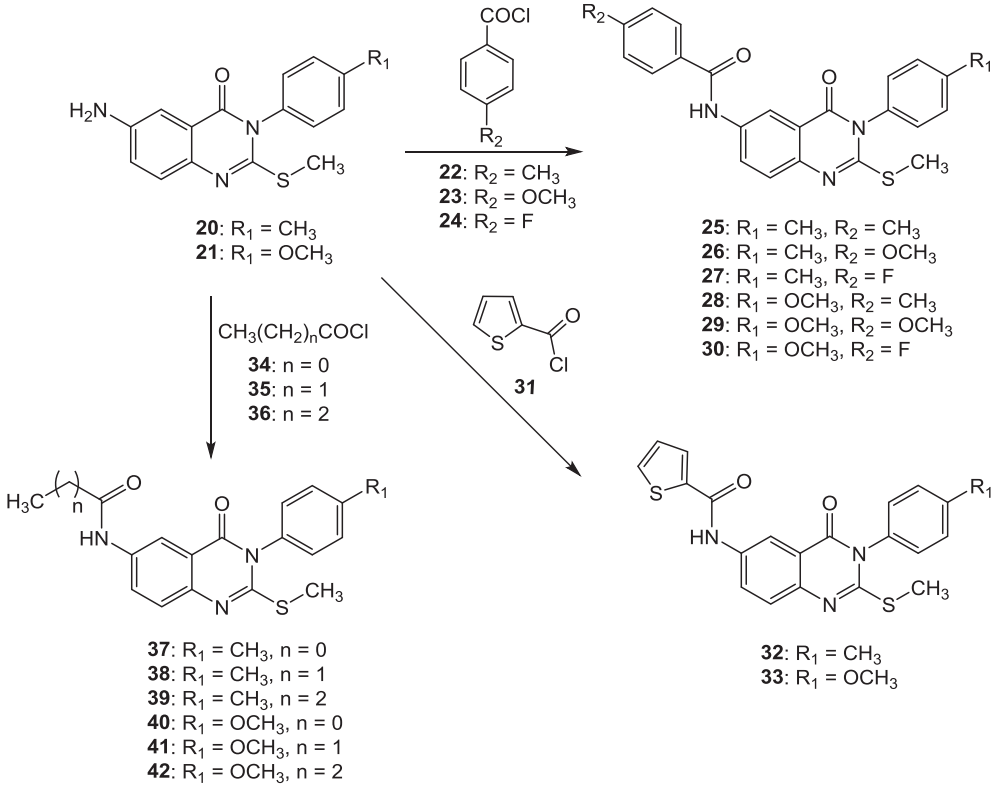

Scheme 2. Synthesis of the target compounds **25–30**, **32**, **33** and **37–42**.

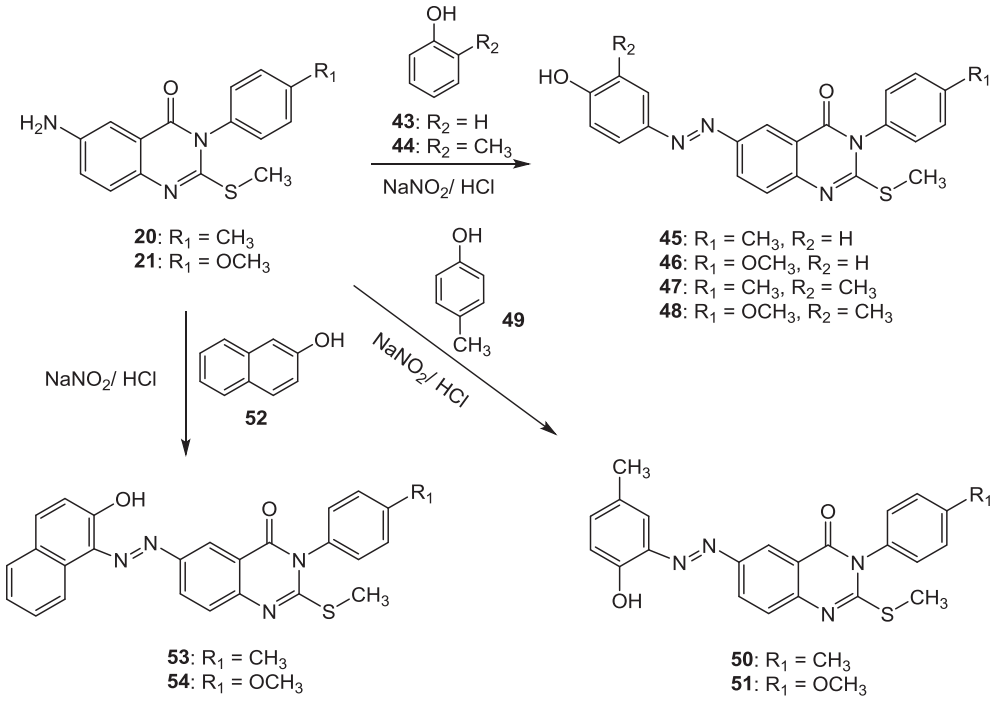

Scheme 3. Synthesis of the target compounds **45–48**, **50**, **51**, **53** and **54**.

and Hela epithelioid carcinoma. Methotrexate (**1**) was used as a standard anticancer drug (IC_{50} 19.26 μM). Cytotoxicity was expressed as the concentration that caused 50% loss of the cell monolayer (IC_{50}), Table 1. The tested compounds exhibited cytotoxic antitumor potency of various magnitudes. Compounds **21**, **53** and **60** showed remarkable broad spectrum cytotoxic potency and considered to be the most active members in this study with average IC_{50} values of 6.7, 7.6 and 9.1 μM, respectively. Compounds **17**, **20**, **54**, **57**, **59** and **61** showed strong activities with average IC_{50} values of 10.5, 13.7, 17.1, 11.8, 18.9, 19.9 μM, respectively. Meanwhile, some of the tested compounds showed selective potency toward certain tumor cell lines, such as **37**, **51**, **56** and **58** against Hela epithelioid carcinoma (15.33 ± 1.6, 24.46 ± 2.0, 12.88 ± 1.5, 20.49 ± 1.8 μM, respectively); **46** against colorectal HCT-116 (24.10 ± 2.0 μM); **45**, **47**, **57** and **61** against both colorectal HCT-116 (16.14 ± 1.5, 18.82 ± 1.7, 8.77 ± 0.9, 15.49 ± 1.4 μM, respectively) and Hela epithelioid carcinoma (28.82 ± 2.1, 18.75 ± 1.6, 7.84 ± 0.9, 12.42 ± 1.3 μM, respectively); **59** against breast MCF-7, prostate PC3 and Hela epithelioid carcinoma (18.07 ± 1.5, 18.94 ± 1.6, 10.62 ± 1.0 μM, respectively); **60** against colorectal HCT-116, breast MCF-7 and Hela cells (8.01 ± 0.8, 8.70 ± 0.6, 5.48 ± 0.7 μM, respectively).

Anticancer drugs usually induce cytotoxicity *via* apoptosis through activation of signaling pathways leading to G2/M arrest [35]. MTT cell viability assay was performed [36–38] using mutant Hela cell line and **59** (cytotoxicity IC_{50} value of 10.62 μM). The flow cytometry experiment results for cell cycle analysis indicated that **59** increased the percentage of apoptotic cells at Pre-G1 phase from 1.91% to 26.59%; increased the percentage of cells at G2/M phase from 6.3% to 44.01%; decreased the percentage of cells in the S phase from 35.09% to 26.44% and decreased the percentage of cells in G0/G1 phase from 58.61% to 29.55% causing cell cycle arrest (Fig. 3). Cell viability assay was also performed for **61** using the mutant HCT-116 cell line which exhibited strong cytotoxicity with IC_{50} values of 15.49 μM. The flow cytometry experiment results for cell cycle analysis indicated that **61** increased the percentage of apoptotic cells in Pre-G1 phase from 1.66% to 18.41%; increased the percentage of cells in G2/M phase from 8.84% to 31.77%; decreased the percentage of cells in the S phase from 39.27% to 29.52% and decreased the percentage of cells in G0/G1 phase from 51.89% to 38.71% causing cell cycle arrest (Fig. 4).

2.2.2. Dihydrofolate reductase (DHFR) inhibition

As an attempt to reveal the antitumor potency mode of action, DHFR inhibition activity was evaluated. The synthesized compounds **16–21**, **25–30**, **32**, **33**, **37–42**, **45–48**, **50**, **51**, **53**, **54** and **56–61** were subjected to Dihydrofolate reductase inhibition evaluation assay using reported procedure, bovine liver DHFR enzyme was used in the test due

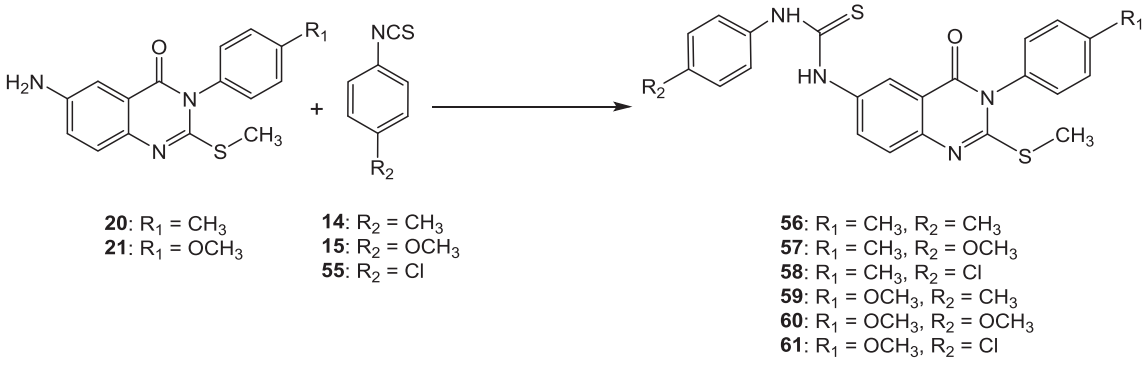

Scheme 4. Synthesis of the target compounds **56–61**.

Table 1
In vitro antitumor assay and DHFR inhibition results (IC_{50} μM) of **16–21**, **25–30**, **32**, **33**, **37–42**, **45–48**, **50**, **51**, **53**, **54**, and **56–61**.

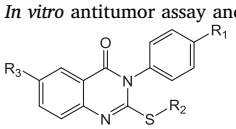

16-21

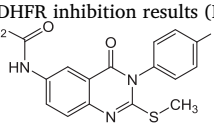

25-30, 32, 33, 37-42

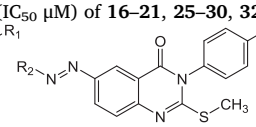

45-48, 50, 51, 53, 54

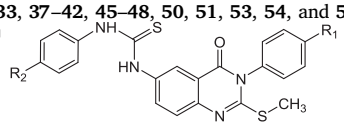

56-61

Compound	R_1	R_2	R_3	*In vitro* Cytotoxicity (IC_{50}, μM)				Average cytotoxicity (IC_{50}, μM)	DHFR inhibition (IC_{50} μM), n = 3
				HCT-116	MCF-7	PC3	Hela		
MTX (**1**)	–	–	–	9.25 ± 0.7	25.32 ± 1.6	28.78 ± 1.8	13.69 ± 1.1	19.3	0.08 ± 0.005
16	CH_3	H	NO_2	92.90 ± 5.1	> 100	> 100	> 100	98.2	15.0 ± 1.98
17	CH_3O	H	NO_2	11.84 ± 1.2	9.97 ± 0.8	13.02 ± 1.0	7.25 ± 0.8	10.5	12.9 ± 0.97
18	CH_3	CH_3	NO_2	39.34 ± 3.2	47.72 ± 3.5	57.76 ± 3.6	40.21 ± 2.9	46.3	18.6 ± 1.78
19	CH_3O	CH_3	NO_2	63.09 ± 4.5	83.47 ± 5.0	89.66 ± 5.5	97.34 ± 5.6	83.4	10.8 ± 1.28
20	CH_3	CH_3	NH_2	10.88 ± 1.0	16.32 ± 1.3	18.21 ± 1.5	9.30 ± 0.9	13.7	9.6 ± 0.87
21	CH_3O	CH_3	NH_2	7.66 ± 0.6	5.73 ± 0.4	9.45 ± 0.8	3.87 ± 0.4	6.7	10.9 ± 0.93
25	CH_3	4-$(CH_3)C_6H_4$	–	51.03 ± 3.9	67.83 ± 4.5	68.07 ± 4.3	71.16 ± 4.1	64.5	18.7 ± 1.45
26	CH_3	4-$(CH_3O)C_6H_4$	–	59.48 ± 4.3	72.47 ± 4.8	76.40 ± 4.5	81.33 ± 4.7	72.4	15.0 ± 1.78
27	CH_3	4-FC_6H_4	–	48.95 ± 3.8	71.72 ± 4.6	76.76 ± 4.9	76.77 ± 4.3	68.6	45.6 ± 2.36
28	CH_3O	4-$(CH_3)C_6H_4$	–	53.73 ± 4.0	75.53 ± 4.8	82.94 ± 5.0	84.36 ± 4.9	74.1	32.9 ± 2.94
29	CH_3O	4-$(CH_3O)C_6H_4$	–	48.18 ± 3.7	64.31 ± 4.4	62.79 ± 4.0	64.47 ± 3.9	59.9	0.2 ± 0.003
30	CH_3O	4-FC_6H_4	–	54.93 ± 4.1	83.25 ± 4.9	89.24 ± 5.3	94.91 ± 5.1	80.6	48.9 ± 2.98
32	CH_3	2-thienyl	–	42.93 ± 3.2	57.20 ± 3.8	61.41 ± 3.9	51.70 ± 3.3	53.3	20.9 ± 1.06
33	CH_3O	2-thienyl	–	44.46 ± 3.5	60.89 ± 3.9	71.26 ± 4.4	63.31 ± 3.6	60.0	0.2 ± 0.001
37	CH_3	CH_3	–	20.56 ± 1.9	27.65 ± 1.8	36.20 ± 2.8	15.33 ± 1.6	24.9	36.8 ± 2.84
38	CH_3	CH_3CH_2	–	67.32 ± 4.4	80.20 ± 4.9	87.52 ± 5.1	86.52 ± 5.0	80.4	38.8 ± 2.56
39	CH_3	$CH_3(CH)_2$	–	42.20 ± 3.3	54.94 ± 3.7	53.78 ± 3.5	51.38 ± 3.1	50.6	40.7 ± 3.78
40	CH_3O	CH_3	–	83.46 ± 4.7	92.59 ± 5.5	> 100	> 100	94.0	> 100
41	CH_3O	CH_3CH_2	–	83.77 ± 4.9	> 100	> 100	> 100	95.9	> 100
42	CH_3O	$CH_3(CH)_2$	–	72.01 ± 4.5	88.81 ± 5.3	97.03 ± 5.7	> 100	89.5	> 100
45	CH_3	4-$(HO)C_6H_4$	–	16.14 ± 1.5	43.93 ± 2.7	48.88 ± 3.1	28.82 ± 2.1	34.4	10.3 ± 1.25
46	CH_3O	4-$(HO)C_6H_4$	–	24.10 ± 2.0	44.84 ± 2.9	52.68 ± 3.4	30.15 ± 2.3	37.9	13.0 ± 1.26
47	CH_3	4-(HO)-3-$(CH_3)C_6H_3$	–	18.82 ± 1.7	31.15 ± 2.1	35.28 ± 2.5	18.75 ± 1.6	26.0	15.3 ± 0.98
48	CH_3O	4-(HO)-3-$(CH_3)C_6H_3$	–	27.02 ± 2.2	36.02 ± 2.3	45.48 ± 3.1	23.04 ± 1.9	32.9	> 100
50	CH_3	2-(HO)-5-$(CH_3)C_6H_3$	–	37.01 ± 3.0	46.19 ± 3.3	47.98 ± 3.3	34.05 ± 2.4	41.3	23.6 ± 2.12
51	CH_3O	2-(HO)-5-$(CH_3)C_6H_3$	–	34.47 ± 2.8	40.27 ± 2.6	41.90 ± 2.9	24.46 ± 2.0	35.3	1.3 ± 0.002
53	CH_3	2-(HO)-1-naphthalenyl	–	6.58 ± 0.4	8.39 ± 0.6	10.60 ± 0.9	4.89 ± 0.5	7.6	57.3 ± 4.58
54	CH_3O	2-(HO)-1-naphthalenyl	–	13.94 ± 1.2	20.28 ± 1.7	22.87 ± 1.8	11.49 ± 1.1	17.1	49.6 ± 2.79
56	CH_3	CH_3	–	32.03 ± 2.5	26.19 ± 1.8	26.39 ± 1.9	12.88 ± 1.5	24.4	2.6 ± 0.87
57	CH_3	CH_3O	–	8.77 ± 0.9	14.09 ± 1.1	16.59 ± 1.3	7.84 ± 0.9	11.8	5.9 ± 0.25
58	CH_3	Cl	–	32.66 ± 2.7	32.50 ± 2.3	33.26 ± 2.4	20.49 ± 1.8	29.7	0.9 ± 0.007
59	CH_3O	CH_3	–	28.16 ± 2.4	18.07 ± 1.5	18.94 ± 1.6	10.62 ± 1.0	18.9	0.3 ± 0.003
60	CH_3O	CH_3O	–	8.01 ± 0.8	8.70 ± 0.6	14.36 ± 1.2	5.48 ± 0.7	9.1	43.6 ± 3.58
61	CH_3O	Cl	–	15.49 ± 1.4	23.12 ± 1.8	28.65 ± 2.1	12.42 ± 1.3	19.9	0.3 ± 0.001

to its structure similarity to that of human DHFR [39–41]. Results were reported as IC_{50} values (Table 1). Methotrexate (**1**) was used as reference drug (IC_{50} 0.08 μM). Compounds **29**, **33**, **59** and **61** proved to be the most active DHFR inhibitors in this study with IC_{50} values of 0.2, 0.2, 0.3 and 0.3 μM, respectively. Compounds **51** and **56–58** showed moderate activity with IC_{50} 1.3, 2.6, 5.9 and 0.9 μM, respectively. Compounds **16–21**, **25**, **26** and **45–47** proved to be of slight activity with IC_{50} 15.0, 12.9, 18.6, 10.8, 9.6, 10.9, 18.7, 15.0, 10.3, 13.0 and 15.3 μM, respectively. The rest of the tested compounds were inactive especially compounds **40–42** and **48** with IC_{50} more than 100 μM.

3. Structure activity relationship

Two main series of compounds were investigated, namely: 3-(4-*methyl*-phenyl)- and 3-(4-*methoxy*-phenyl)-quinazolin-4(3*H*)-one for their antitumor activity and DHFR inhibition. *In regard to antitumor activity,* the starting material **17** showed remarkable antitumor potency with average IC_{50} values of 10.5 μM. Reduction of the 6-nitro groups gave the 6-amino derivatives **20** and **21** (average IC_{50} values of 13.7 and 6.7 μM, respectively) with enhanced antitumor potency. Acylation of the 6-amino functions with a collection of acid chlorides produced the corresponding amides which proved to be devoid of antitumor potency. Diazotization of the 6-amino functions of **20** and **21** with a collection of phenols gave the corresponding diazenyl analogues with marginal antitumor activity except 6-[(2-Hydroxy-naphthalen-1-yl) diazenyl]-2-(methyl-thio)-3-(4-methyl-phenyl)-quinazolin-4(3*H*)-one (**53**) and 6-[(2-Hydroxy-naph-thalen-1-yl)diazenyl]-3-(4-methoxy-phenyl)-2-(methyl-thio)quina-zolin-4(3*H*)-one (**54**) which showed remarkable antitumor potency with average IC_{50} values of 7.6 and 17.1 μM, respectively. The 6-amino functions of **20** and **21** were further utilized to produce the thiourea analogues 1-(4-Methoxy-phenyl)-3-(2-(methyl-thio)-4-oxo-3-(4-methyl-phenyl)-3,4-di-hydro-quinazolin-6-yl) thiourea (**57**), 1-(3-(4-Methoxy-phenyl)-2-(methyl-thio)-4-oxo-3,4-di-hydro-quinazolin-6-yl)-3-(4-methyl-phenyl)thiourea (**59**) and 1-(4-Methoxy-phenyl)-3-(3-(4-methoxy-phenyl)-2-(methyl-thio)-4-oxo-3,4-di-hydro-quinazolin-6-yl)-thiourea (**60**) which showed remarkable antitumor activity with average IC_{50} values of 11.8, 18.9 and 9.1 μM, respectively. *In regard to DHFR inhibition activity,* the starting materials 2-mercapto-3-(4-substituted-phenyl)-6-nitro-quinazolin-4(3*H*)-ones (**16** and **17**) showed marginal DHFR inhibition activity with IC_{50} values of 15.0 and 12.9 μM, respectively. Methylation of the 2-mercapto functions produced **18** and **19** (IC_{50} values of 18.6 and 10.8 μM, respectively), or reduction of the 6-nitro groups gave the 6-amino derivatives **20** and **21** (IC_{50} values of 9.6 and 10.9 μM, respectively) without sensible enhancement of the DHFR inhibition activity. Acylation of the 6-amino functions of **20** and **21** with a collection of substituted aromatic,

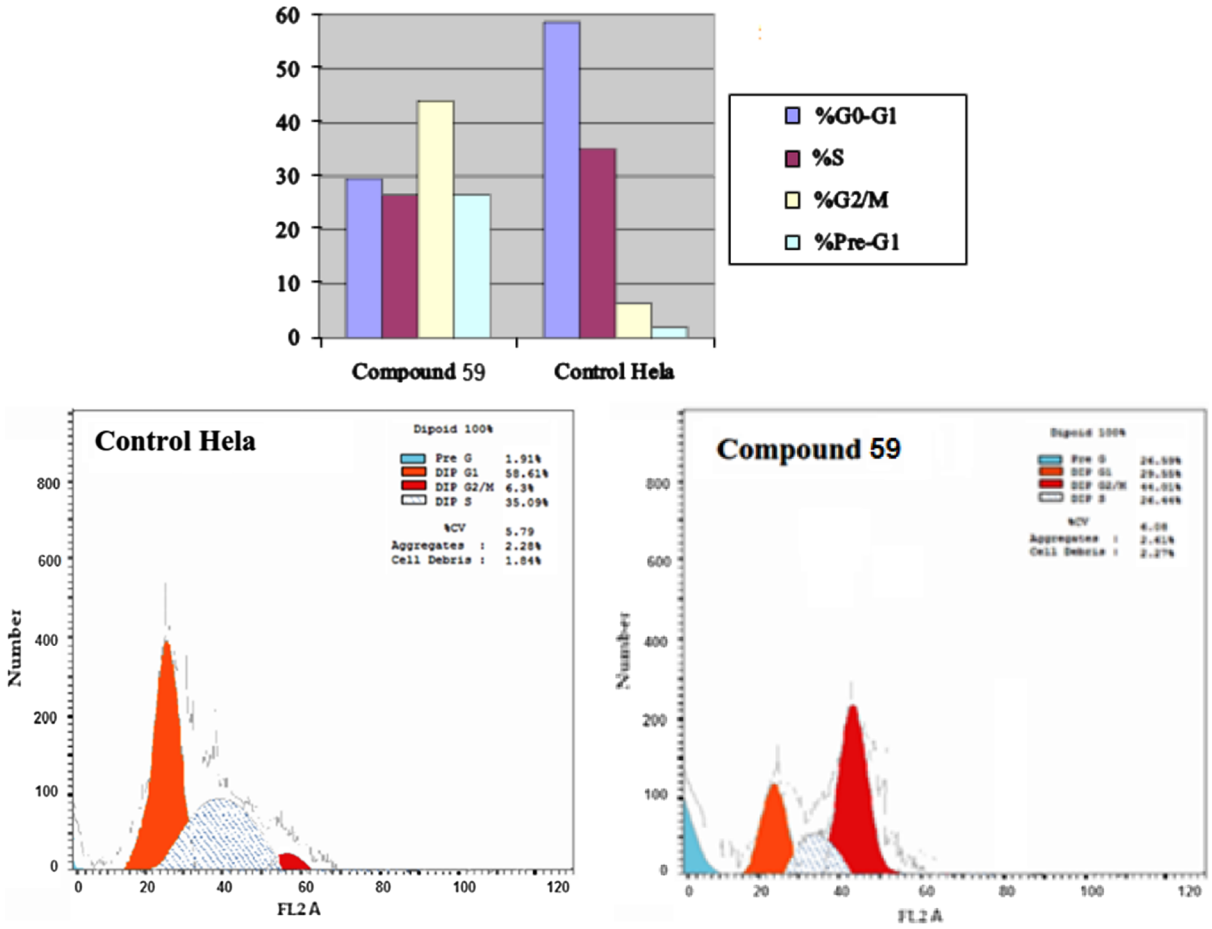

Fig. 3. Cell cycle analysis and apoptosis effect in Hela cell line treated with **59** against control Hela cell line (upper panel), which evaluated by flow cytometry (lower panel).

heterocyclic or aliphatic acid chlorides produced the corresponding amides with marginal DHFR inhibition activity except compounds 4-methoxy-*N*-(3-(4-methoxy-phenyl)-2-(methyl-thio)-4-oxo-3,4-dihydro-quinazolin-6-yl)benzamide (**29**) and *N*-(3-(4-methoxy-phenyl)-2-(methyl-thio)-4-oxo-3,4-dihydro-quinazolin-6-yl)thiophene-2-carboxamide (**33**) which showed remarkable potency with IC_{50} values of 0.2 μM each. Aromatic and heterocyclic amides at position 6- of the quinazoline nucleus contributed to the antifolate potency more than aliphatic amides. Meanwhile, the combination of 6-(aromatic or heterocyclic)-amides and 3-(4-methoxy-phenyl)- favor the activity rather than the combination of 6-(aliphatic)-amides and 3-(4-methyl-phenyl)-quinazoline. Diazotization of the 6-amino functions of **20** and **21** with variety of phenols gave the corresponding diazenyl analogues with marginal DHFR inhibition activity except 6-[(2-Hydroxy-5-methyl-phenyl)diazenyl]-3-(4-methoxy-phenyl)-2-(methyl-thio)quinazolin-4(3*H*)-one (**51**) which showed moderate DHFR inhibition potency with IC_{50} values of 1.3 μM. The 6-amino functions of **20** and **21** were further utilized to produce the thiourea analogues **56–61** with moderate inhibition activity except 1-(3-(4-Methoxy-phenyl)-2-(methyl-thio)-4-oxo-3,4-dihydro-quinazolin-6-yl)-3-(4-methyl-phenyl)-thiourea (**59**) and 1-(4-Chloro-phenyl)-3-(3-(4-methoxy-phenyl)-2-(methyl-thio)-4-oxo-3,4-dihydro-quinazolin-6-yl)-thiourea (**61**) which expressed considerable DHFR inhibition potency with IC_{50} values of 0.3 μM each. Generally, the 3-(4-*methoxy*-phenyl)- series favor the DHFR inhibition activity rather than 3-(4-*methyl*-phenyl)-quinazolin-4(3*H*)-one.

4. Molecular modeling simulation study

Molecular modeling methods [42,43] were used to get a better understanding about the molecular structure behavior of the most active DHFR inhibtor **29** and the least active **48**, in comparison to methotrexate (MTX, **1**). Conformational analysis was performed using MMFF94 force-field (RMS gradient of 0.01 kcal/Å mol) implemented in MOE 2009.10 [44,45]. The lowest energy conformers for **1**, **29** and **48** were shown in Fig. 5. Molecular docking was performed for the binding pocket of human dihydrofolate reductase binding domain which is in tertiary complex with dihydronicotinamide adeninedinucleotide phosphate (NADPH) and **1**, (code ID 1DLS) to predict the binding affinity of the newly synthesized compounds as hDHFR inhibitors [46].

Fig. 6 illustrates the 2D binding mode of **1**, **29** and **48**. The obtained docking data showed that the binding of **1** to hDHFR is expressed as a complex interaction where the receptor site undergo a kind of isomerizational change leading to the tight binding with hydrogen bonding of the central amide carbonyl function as hydrogen bond acceptor (HBA) to Thr56 and Ser59.

MTX (**1**) binds also through hydrogen and ionic bonding with Lys55, arene-arene interaction with Phe34 and Phe31 amino acid residues (Fig. 6a). The most active **29** showed high affinity binding toward the amino acid residues Thr56, Ser59 and Ser118 as hydrogen bonding acceptor (Fig. 6b); which is more or less the same fashion and type of binding as the reference **1** do. This could be the reason for the remarkable activity of **29** with IC_{50} 0.2 ± 0.003 μM. On the other hand, **48** (IC_{50} > 100 μM) did not bind with those amino acid residues and the S-methyl and part of the terminal phenyl groups were exposed out the enzyme pocket explaining its poor activity (Fig. 6c). Further modeling studies and docking comparisons between structurally related compounds were done to uncover the reason behind the unique activity of **29** and the modest potency of the other closely related analogs.

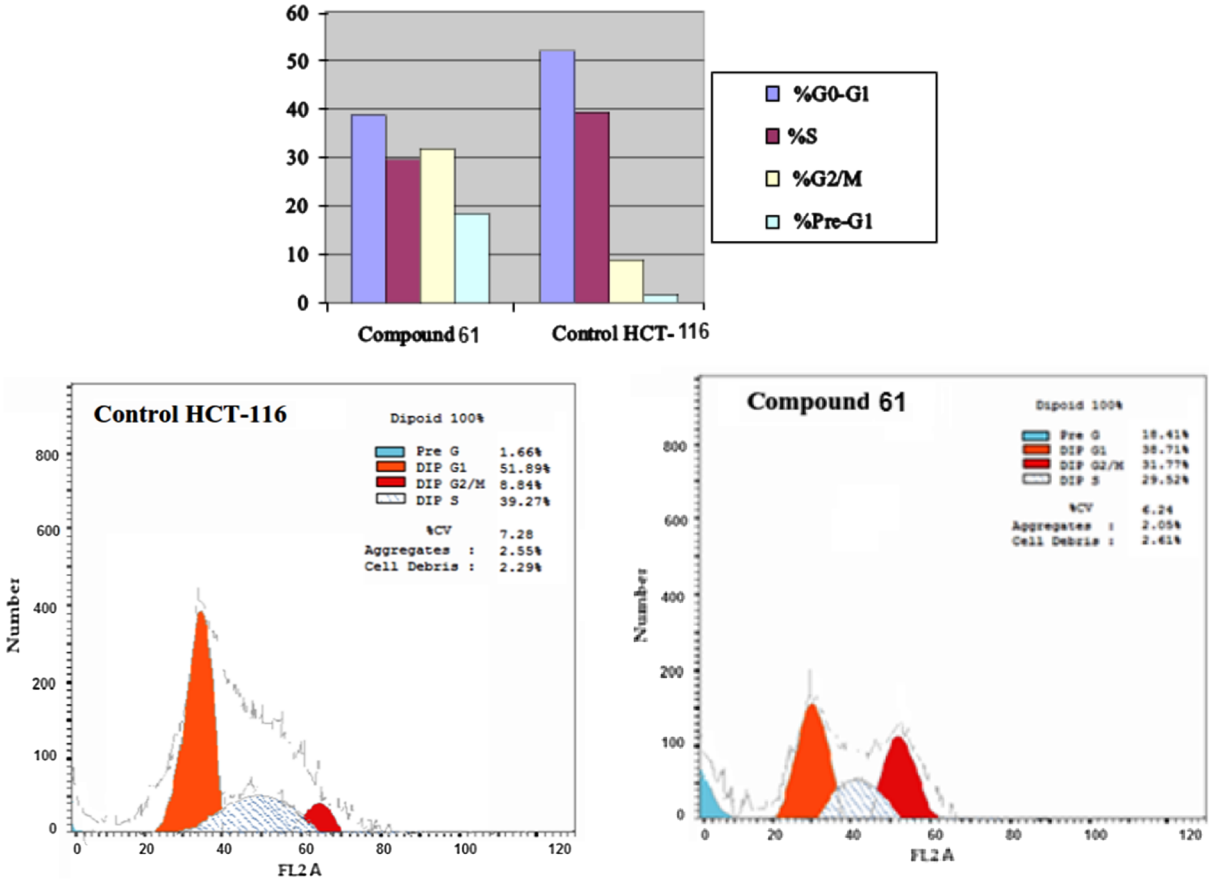

Fig. 4. Cell cycle analysis and apoptosis effect in HCT-116 cell line treated with **61** against control HCT-116 cell line (upper panel), which evaluated by flow cytometry (lower panel).

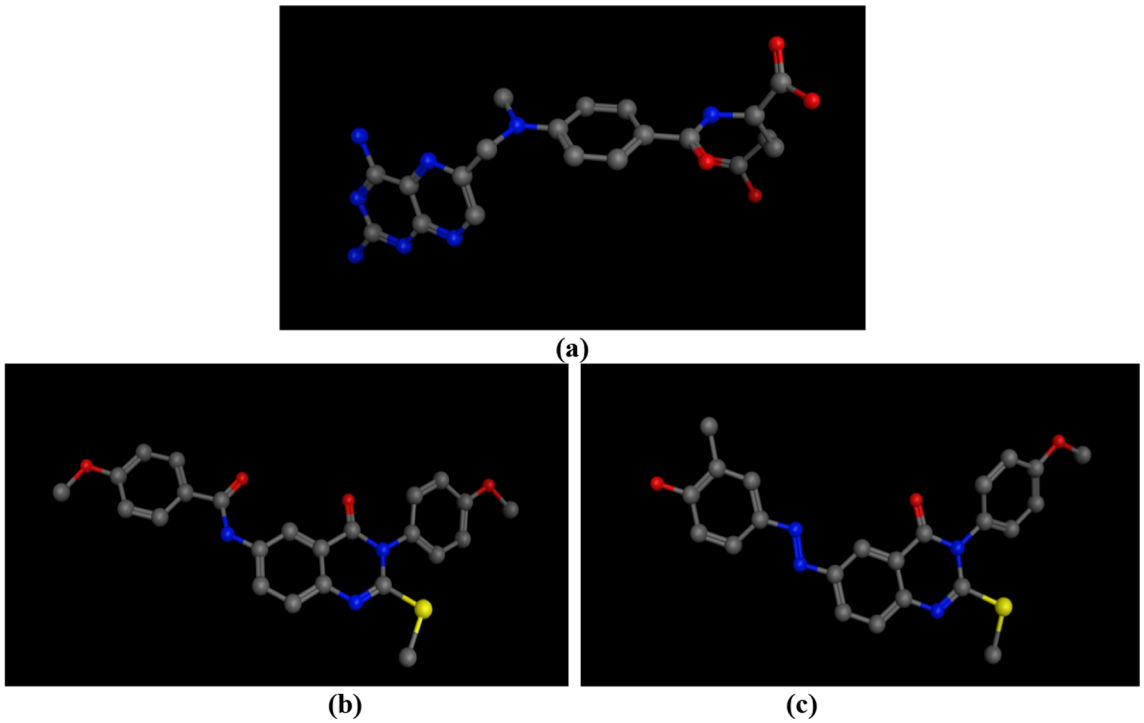

Fig. 5. The lowest energy conformer of (a) MTX **1**, (b) the most active **29** (c) and the least active **48** with balls and cylinders.

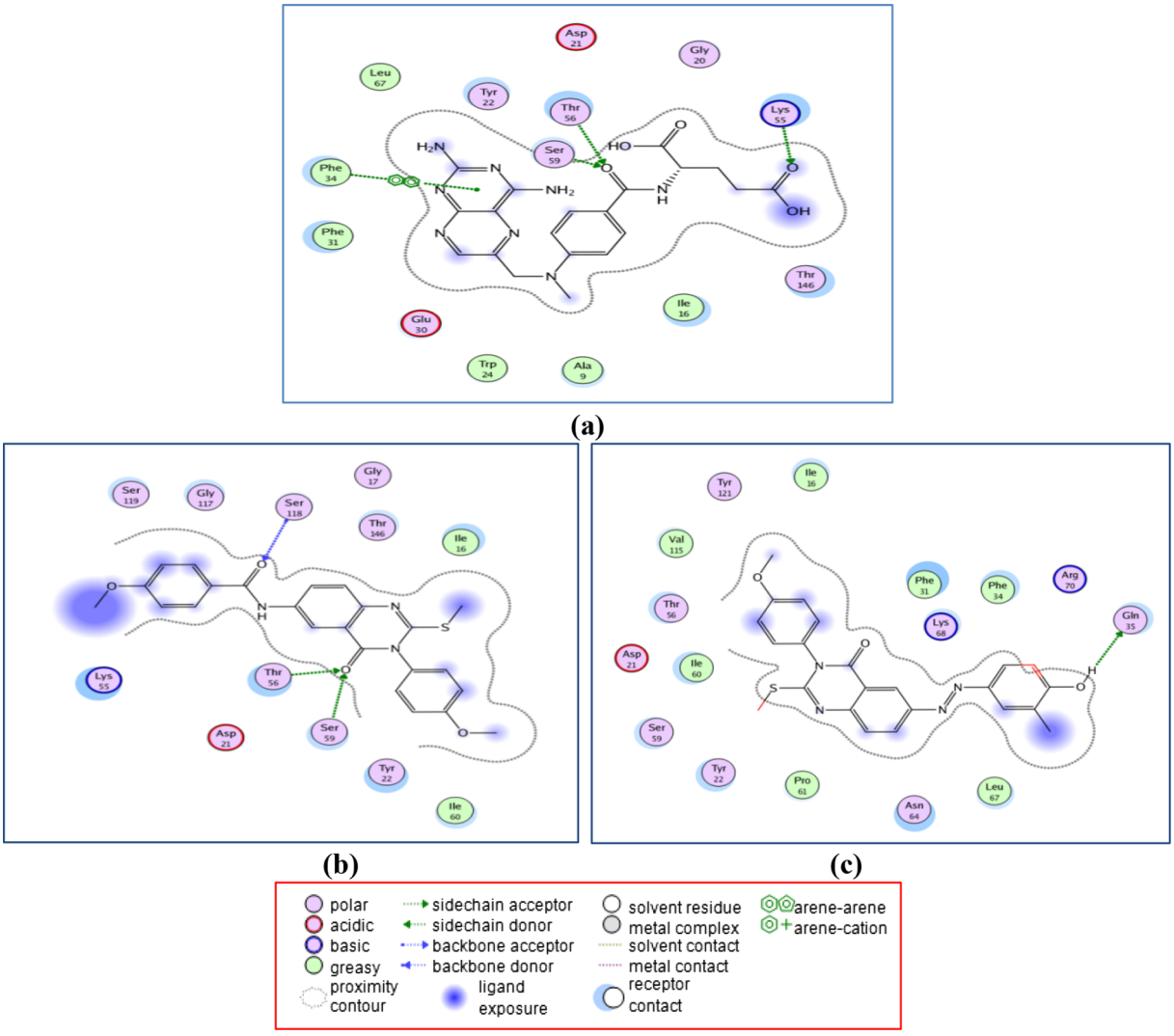

Fig. 6. 2D binding mode and residues involved in the recognition of (a) MTX (**1**, IC_{50} 0.08 μM), (b) the most active compound **29** (IC_{50} 0.2 ± 0.003 μM), and (c) the least active compound **48** (IC_{50} > 100 μM) docked and minimized in the hDHFR binding pocket.

Comparison of **26** (IC_{50} 15.0 ± 1.78 μM) and **29** (IC_{50} 0.2 ± 0.003 μM) was performed to predict the reason of the efficacy difference. The structure difference was the 4-methoxy-phenyl group in **29** instead of 4-methyl-phenyl group in **26**. This difference led to the change of orientation and the binding poses inside the pocket. Compound **26** lacked the essential binding toward the amino acid residues Thr56 and Ser59 to which **29** bonded, in addition to the arene-arene interaction with Phe31. The same analogy was adopted to compare **32** (IC_{50} 20.9 ± 1.06 μM) and **33** (IC_{50} 0.2 ± 0.001 μM).

Comparison of the equipotent compounds **29** and **33** (IC_{50} 0.2 μM); revealed that the structure difference lies in the 4-methoxy-phenyl-carboxamide group in **29** and 2-thienyl-carboxamide group in **33**. This structure difference did not affect the orientation and the binding poses inside the enzyme pocket. The same could be applied for **47** (15.38 ± 0.98 μM) and **48** (> 100 μM); **50** (23.6 ± 2.12 μM) and **51** (1.3 ± 0.002 μM); **48** (> 100 μM) and **51** (1.3 ± 0.002 μM).

Additional ligands docking and alignment inside hDHFR binding pocket was performed [47]. The binding pocket surface map was calculated showing MTX (**1**) occupying the whole space lying into the groove pocket (Fig. 7a). Compound **29** pocket alignments showed a similar pattern filling the area of the active site with its bulkiness, forming favorable binding contacts (Fig. 7b). On the other hand, the structure of **48** was exposed out the surface wall of the active site explaining its poor DHFR inhibitory activity (Fig. 7c).

Flexible Alignment computational procedures were performed using MOE/MMFF94 flexible alignment tool [48–50]. 100 conformers of each compound were generated and minimized with a distance-dependent dielectric model. Fig. 8a showed that the most active compounds **29**, **33**, **59** and **61** are perfectly aligned especially at the quinazoline moiety. Fig. 8b showed that the least active compounds **40–42** and **48** are aligned well especially at the quinazoline moiety. Fig. 8c showed that the least active compounds are completely deviated from the most active counterparts.

Surface mapping comparison of **29**, **48** and MTX (**1**) was performed to detect their surface properties and the similarity in the position of hydrophilic and hydrophobic sites that bind to the active sites (Fig. 9), [51]. As noticed in Fig. 9a and b, it is clear that there is similarity in the positions of the hydrophilic site at the two sides of the structure and in the presence of hydrophobic aromatic ring in the center of the molecule, in addition to the obvious similarity between the pteridine ring in MTX (**1**) and quinazoline ring in the newly synthesized compounds.

Lipinski's rule of five is a rule of thumb to determine the drug likeness or investigating the properties that would make a chemical compound with a certain pharmacological or biological activity likely orally active drug in humans [52–54]. As a part of the molecular modeling study, the compliance of the most active newly synthesized compounds **29**, **33**, **59** and **61** to the Lipinski rule of five was checked as illustrated in Table 2. It can be observed that all of the active

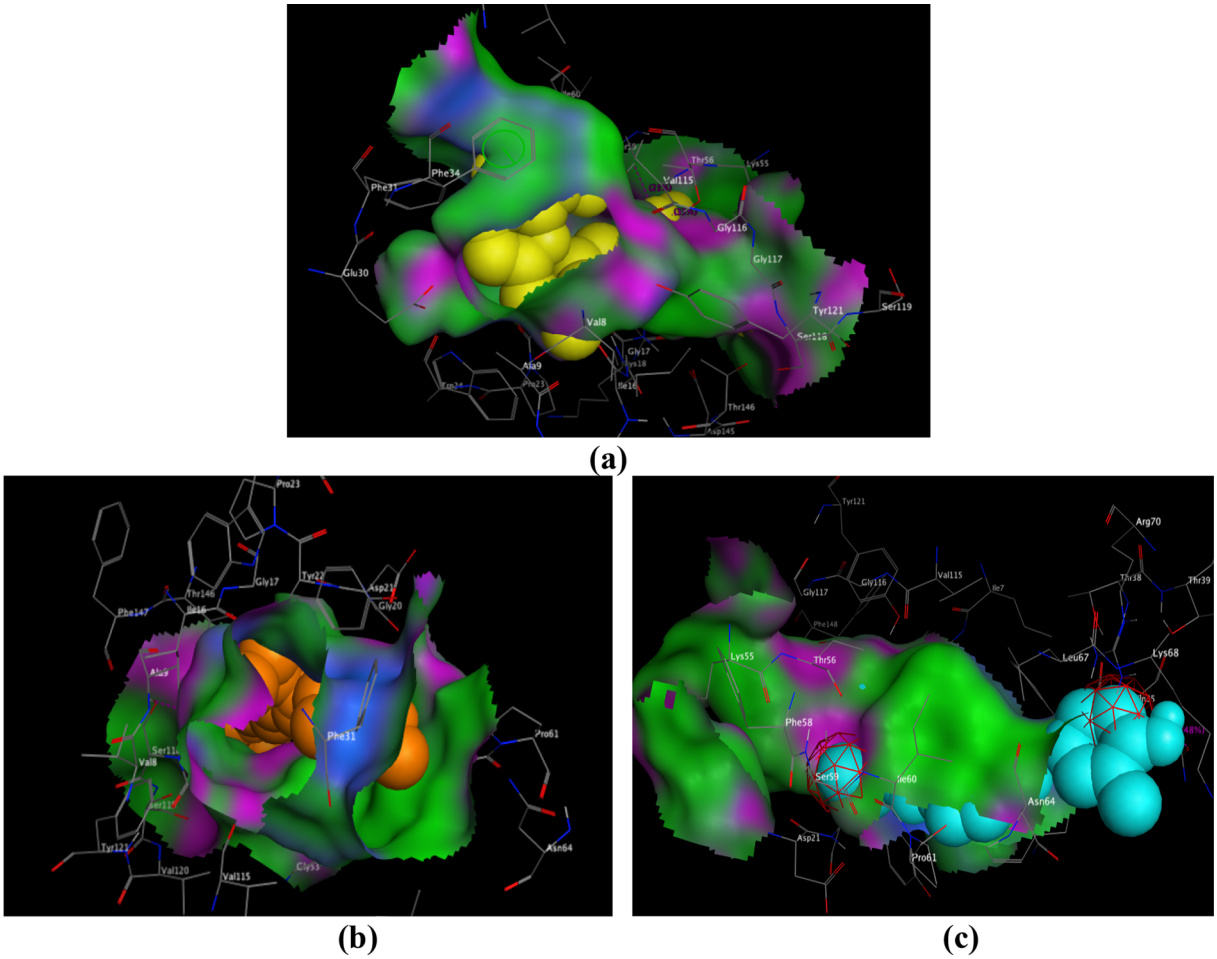

Fig. 7. The aligned conformations of (a) MTX (**1**, space filled yellow, IC_{50} 0.08 μM), (b) the most active **29** occupying the DHFR binding pocket (space filled orange, IC_{50} 0.2 ± 0.003 μM) and (c) the most inactive **48** (space filled cyan, IC_{50} > 100 μM) exposing out of the DHFR binding pocket surface map.

compounds obey Lipinski's rule of five.

The pharmacokinetics ADMET property limitations [55–57] for the active compounds were calculated. The ADMET data were predicted and showed in Table 3. Based on the predicted values of the most active compounds **29**, **33**, **59** and **61**, the new compounds have comparable ADMET data with that of **1.** The active compounds are capable of penetrating blood brain barrier (BBB) and can be absorbed by intestine. Their estimated log S values are −4, which indicate low water solubility. All active compounds are expected to be non-substrate/non-inhibitors of CYP 2D6 enzyme which suggests low possibility of drug-drug interaction occurrence. Furthermore, toxicity tests data showed that all of the compounds are non-toxic nor-mutagenic in Ames test and all are non-carcinogenic.

5. Conclusion

Two main series of compounds were investigated, namely: 3-(4-***methyl***-phenyl)- and 3-(4-***methoxy***-phenyl)-quinazolin-4(3*H*)-ones. Compounds **21**, **53** and **60** showed broad spectrum remarkable cytotoxic potency and considered to be the most active members in this study with average IC_{50} values of 6.7, 7.6 and 9.1 μM, (Fig. 10). MTT cell viability assay was performed using the mutant Hela, the mutant HCT-116 cell lines against compound **59** and **61**, respectively. Both compounds induced their cytotoxicity via Pre-G1 apoptosis and inhibited cell growth at G2-M. Compounds **29**, **33**, **59** and **61** proved to be the most active DHFR inhibitors in this study with IC_{50} values of 0.2, 0.2, 0.3 and 0.3 μM, respectively.

The most active DHFR inhibitor **29** showed high affinity binding toward the amino acid residues Thr56, Ser59 and Ser118 as hydrogen bond acceptor. Compounds **29**, **33**, **59** and **61** obeyed Lipinski's rule of five and have comparable ADMET data with that of MTX (**1**).

In the present study, it seemed that compound **21**, **59** and **61** probably exerts its antitumor potency (average IC_{50} values of 6.7, 18.9 and 19.9 μM, respectively) through DHFR inhibition (IC_{50} value of 10.9, 0.3 and 0.3 μM, respectively). The cell cycle analysis gave evidence that compounds **59** and **61** exerted their antitumor activity probably through dual modes, apoptotic behavior and DHFR inhibition. The other active antitumor exerted their potency with some other mechanism(s). The active compounds and their biological results as well as molecular modeling studies could be considered as a template for future investigation and development.

6. Experimental

All melting points (°C) were measured by Stuart melting point apparatus SMP30 and they are uncorrected. ^{1}H, ^{13}C NMR, DEPT-135, 2D COSY and 2D HSQC spectra were recorded on Bruker Avance III HD FT-high resolution- ^{1}H NMR (400 MHz), ^{13}C NMR (100 MHz) at Faculty of Pharmacy-Mansoura University; chemical shifts are expressed in δ ppm with reference to TMS. Mass spectra was carried out on Direct Inlet part to mass analyzer in Thermo Scientific GCMS model ISQ at the Regional Center for Mycology and Biotechnology (RCMB), Al-Azhar University, Nasr City, Cairo. Reaction times were determined using TLC on silica gel plates 60F245 E. Merk, using chloroform/methanol 9:1 or chloroform alone as eluting system and the spots were visualized by UV (366–245 nm). Starting materials and reagents were purchased from

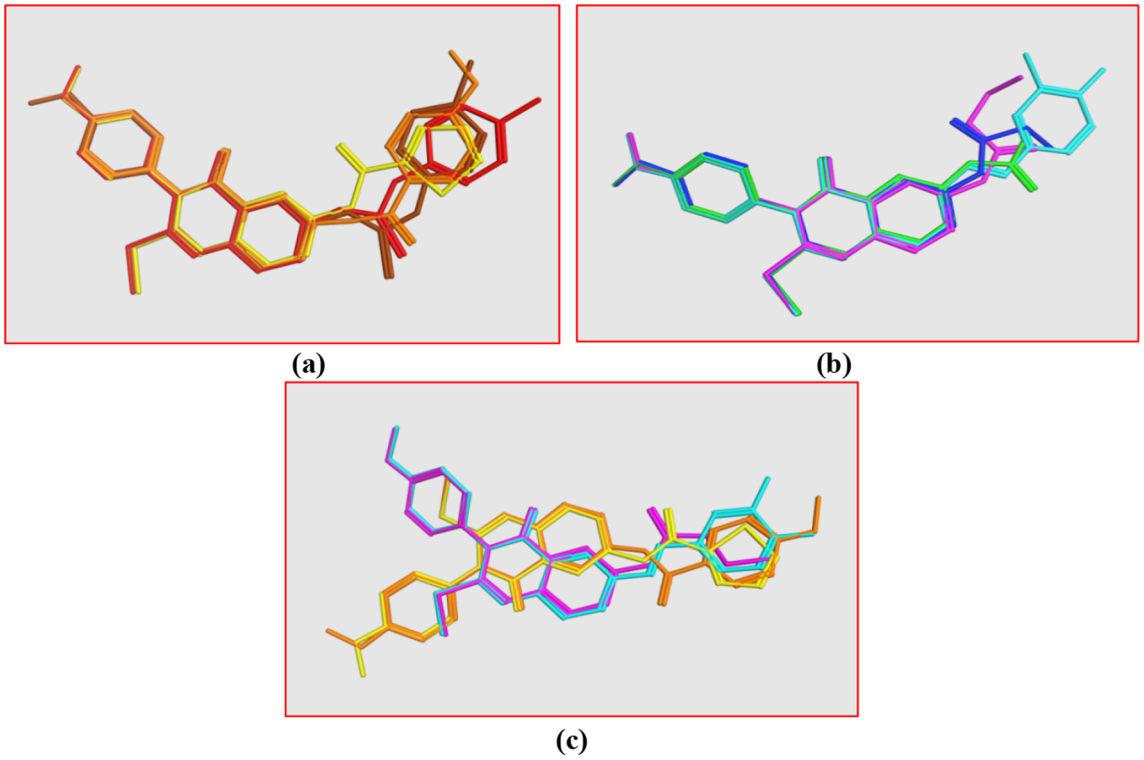

Fig. 8. (a) Flexible alignment of the most active compounds **29** (orange), **33** (yellow), **59** (red) and **61** (brown), (b) Flexible alignment of the least active compounds **40** (green), **41** (blue), **42** (violet) and **48** (cyan), (c) Flexible alignment of the most active compounds **29** (orange) and **33** (yellow) against the least active compounds **42** (violet) and **48** (cyan).

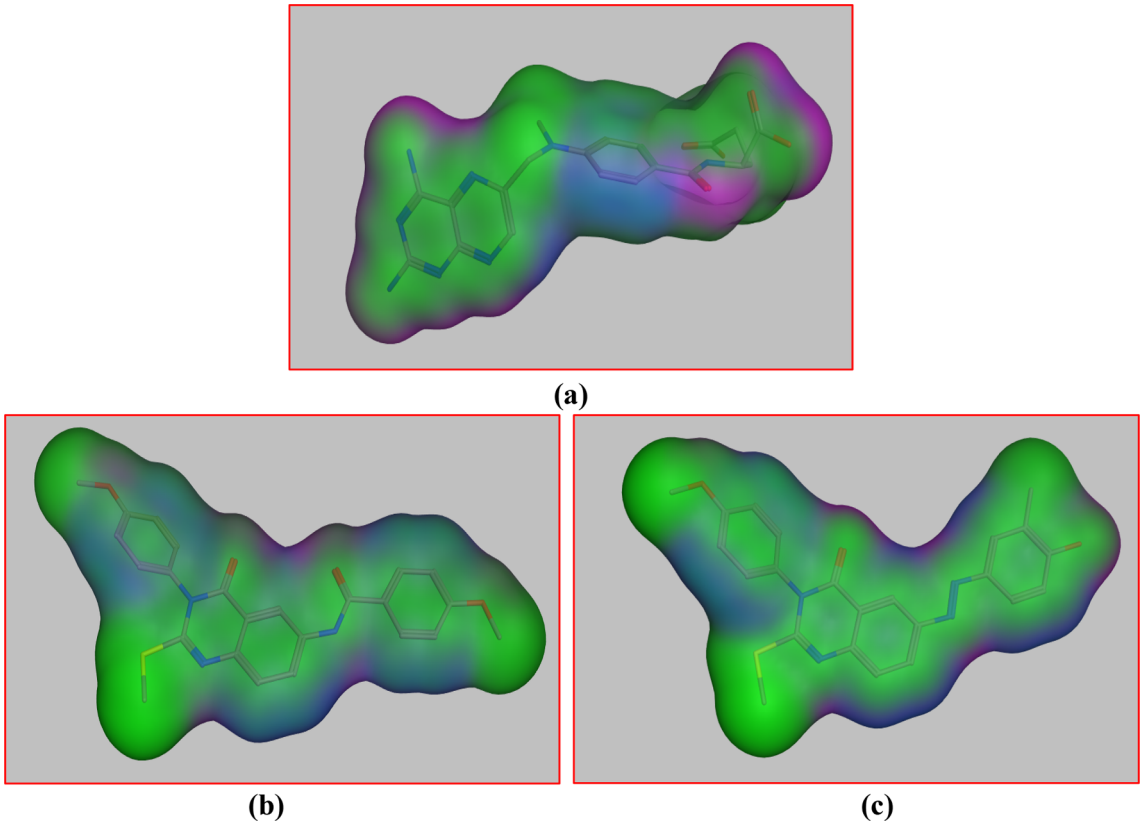

Fig. 9. (a) Surface map for MTX (**1**) in pocket side. (b) Surface map for the most active compound **29** in pocket side. (c) Surface map for the least active compound **48** in pocket side. Pink: hydrophilic, blue: mild polar, green: hydrophobic.

Table 2
Calculated parameters of Lipinski's rule of five for compounds **29**, **33**, **59** and **61**.

Compound	Parameter						*n*Vs[g]
	Log P[a]	TPSA[b]	MW[c]	*n*HBA[d]	*n*HBD[e]	*n*RB[f]	
29	4.97	80.23	447.5	5	1	6	0
33	5.02	71.00	423.52	4	1	5	1
59	5.82	98.05	462.60	4	2	7	1
61	6.17	98.05	483.02	4	2	7	1

[a] Calculated lipophilicity.
[b] Total polar surface area.
[c] Molecular weight.
[d] Number of hydrogen bond acceptor.
[e] Number of hydrogen bond donor.
[f] Number of rotatable bonds.
[g] Number of violation from Lipinski's rule of five.

Sigma-AldrichCo., U.S.A., El-Gomhoria and El-Nasr Pharmaceutical and Chemical Co., Egypt. Dihydrofolate reductase (DHFR) inhibition activity experiments were performed at Pharmacology and Biochemistry Department, Faculty of Pharmacy; Future University in Egypt. *In vitro* antitumor activity was performed in the Department of Pharmacognosy, Faculty of Pharmacy, Mansoura University. Cell Cycle analysis was performed at the confirmatory diagnostic unit, VACSERA, Egypt.

6.1. Chemistry

6.1.1. General procedure for the synthesis of 2-mercapto-3-(4-substituted-phenyl)-6-nitro-quinazolin-4(3H)-ones (**16** and **17**)

A mixture of 5-nitroanthranilic acid (**13**, 0.91 g, 0.005 mol), the appropriate substituted phenylisothiocyanate derivative (**14** or **15**, 0.005 mol), and TEA (2 ml) in ethanol (50 ml) was heated under reflux for 4 h. The reaction mixture was then stirred at room temperature for 12 h. The separated yellow solid was filtered, washed with methanol, dried and recrystallized from ethanol to give **16** and **17**.

*6.1.1.1. 2-Mercapto-6-nitro-3-(4-methyl-phenyl)quinazolin-4(3H)-one (**16**).* Yellowish white crystals (0.93 g, 60%), m.p. 270–2 °C. ^{1}H NMR (DMSO-d_6): δ 3.38 (s, 3H, CH_3Ph), 7.17 (d, 2H, J = 8.4 Hz, ArH), 7.30 (d, 2H, J = 8.4 Hz, ArH), 7.56 (d, 1H, J = 8.8 Hz , ArH), 8.56–8.59 (dd, 1H, J = 2.4, 8.8 Hz, ArH), 8.60 (d, 1H, J = 2.4 Hz, ArH), 13.46 (s, 1H, SH). ^{13}C NMR: δ 21.3, 116.9, 117.6, 124.0, 128.9, 130.1, 130.6, 136.7, 138.3, 143.2, 144.0, 159.3, 177.7. MS (*m/z*, %) for $C_{15}H_{11}N_3O_3S$: (M^+ 313.0, 76.55), 312 (100).

*6.1.1.2. 2-Mercapto-3-(4-methoxy-phenyl)-6-nitroquinazolin-4(3H)-one (**17**).* Yellowish white crystals (1 g, 65%), m.p. 287–90 °C. ^{1}H NMR (DMSO-d_6): δ 3.82 (s, 3H, OCH_3), 7.04 (d, 2H, J = 8.8 Hz, ArH), 7.21 (d, 2H, J = 8.8 Hz, ArH), 7.57 (d, 1H, J = 8.8 Hz , ArH), 8.57–8.60 (dd, 1H, J = 2.4, 8.8 Hz, ArH), 8.61 (d, 1H, J = 2.4 Hz, ArH), 13.46 (s, 1H, SH), ^{13}C NMR: δ 55.8, 114.7, 117.0, 117.6, 124.0, 130.2, 130.6, 131.9, 143.3, 144.0, 159.4, 159.5, 177.9. MS (*m/z*, %) for $C_{15}H_{11}N_3O_4S$: (M^+ 329.0, 70.02), 114 (100).

6.1.2. General procedure for the synthesis of 3-(4-substituted-phenyl)-2-(methyl-thio)-6-nitro-quinazolin-4(3H)-ones (**18** and **19**)

A mixture of the 2-mercapto-quinazoline analog (**16** or **17**, 0.005 mol), methyl iodide (3 ml), and anhydrous potassium carbonate (1 g) in acetone (50 ml) was stirred at room temperature for 8 h. The excess carbonate was filtered off, washed with acetone, the filtrate was then evaporated under vacuum, and the obtained residue was dried, and recrystallized from ethanol to give **18** and **19**.

*6.1.2.1. 2-(Methyl-thio)-6-nitro-3-(4-methyl-phenyl)quinazolin-4(3H)-one (**18**).* White crystals (1.31 g, 80%), m.p. 200–2 °C. ^{1}H NMR ($CDCl_3$): δ 2.40 (s, 3H, CH_3Ph), 2.48 (s, 3H, SCH_3), 7.13 (d, 2H, J = 8.0 Hz , ArH), 7.31 (d, 2H, J = 8.0 Hz, ArH), 7.65 (d, 1H, J = 8.8 Hz, ArH), 8.43–8.46 (dd, 1H, J = 2.4, 8.8 Hz, ArH), 9.02 (d, 1H, J = 2.4 Hz, ArH), ^{13}C NMR: δ 15.8, 21.5, 119.8, 124.2, 127.7, 128.5, 128.8, 130.7, 132.5, 140.9, 144.7, 151.6, 160.6, 163.4. MS (*m/z*, %) for $C_{16}H_{13}N_3O_3S$: (M^+ 327.0, 100).

*6.1.2.2. 3-(4-Methoxy-phenyl)-2-(methyl-thio)-6-nitroquinazolin-4(3H)-one (**19**).* White crystals (1.32 g, 77%), m.p. 230–2 °C. ^{1}H NMR ($CDCl_3$): δ 2.58 (s, 3H, SCH_3), 3.91 (s, 3H, OCH_3), 7.09 (d, 2H, J = 8.8 Hz , ArH), 7.25 (d, 2H, J = 8.8 Hz, ArH), 7.74 (d, 1H, J = 8.8 Hz, ArH), 8.52–8.55 (dd, 1H, J = 2.4, 8.8 Hz, ArH), 9.12 (d, 1H, J = 2.4 Hz, ArH), ^{13}C NMR: δ 15.9, 55.6, 115.2, 119.7, 124.2, 127.5, 127.7, 128.8, 130, 144.7, 151.6, 160.8, 160.9, 163.8. MS (*m/z*, %) for $C_{16}H_{13}N_3O_4S$: (M^+ 343.0, 100).

6.1.3. General procedure for the synthesis of 6-amino-3-(4-substituted-phenyl)-2-(methyl-thio)quinazolin-4(3H)-ones (**20** and **21**)

A mixture of the 6 nitro-quinazoline derivative (**18** or **19**, 0.005 mol) and $SnCl_2{\cdot}2H_2O$ (0.025 mol, 5.64 g), in acetone (50 ml), was heated under reflux for 2 h. the reaction mixture was allowed to cool then poured into ice. The pH was rendered slightly basic (pH 8) by addition of 5% aqueous sodium bicarbonate and the resulting basic mixture was stirred at room temperature for 0.5 hr. The separated solid was filtered, washed with water, and dried. The dried solid was then extracted with acetone, the extract was then evaporated under vacuum, and the obtained residue was dried, and recrystallized from ethanol to give **20** and **21**.

*6.1.3.1. 6-Amino-2-(methyl-thio)-3-(4-methyl-phenyl)quinazolin-4(3H)-one (**20**).* Greyish white crystals (0.89 g, 60%), m.p. 213–5 °C. ^{1}H NMR ($CDCl_3$): δ 2.47 (s, 3H, CH_3Ph), 2.51 (s, 3H, SCH_3), 3.93 (s, 2H, NH_2), 7.11–7.14 (dd, 1H, J = 2.8, 8.4 Hz , ArH), 7.21 (d, 2H, J = 8.0 Hz, ArH), 7.36 (d, 2H, J = 8.0 Hz, ArH), 7.46 (d, 1H, J = 2.8 Hz, ArH), 7.5 (d, 1H, J = 8.4 Hz, ArH), ^{13}C NMR: δ 15.4, 21.4, 109.7, 120.7, 123.3, 127.4, 128.9, 130.3, 133.6, 140.0, 141.2, 144.6, 154.0, 161.9. MS (*m/z*, %) for $C_{16}H_{15}N_3OS$: (M^+ 297.9, 73.80), 89 (100).

*6.1.3.2. 6-Amino-3-(4-methoxy-phenyl)-2-(methyl-thio)quinazolin-4(3H)-one (**21**).* Greyish white crystals (0.98 g, 63%), m.p. 191–3 °C. ^{1}H NMR ($CDCl_3$): δ 2.51 (s, 3H, SCH_3), 3.89 (s, 3H, OCH_3), 3.94 (s, 2H, NH_2), 7.05 (d, 2H, J = 8.0 Hz, ArH), 7.1–7.13 (dd, 1H, J = 2.8, 8.4 Hz , ArH), 7.24 (d, 2H, J = 8.0 Hz, ArH), 7.45 (d, 1H, J = 2.8 Hz, ArH), 7.49 (d, 1H, J = 8.8 Hz, ArH), ^{13}C NMR: δ 15.4, 55.5, 109.7, 114.8, 120.7, 123.3, 127.4, 128.7, 130.3, 141.2, 144.6, 154.3, 160.5, 162.1. MS (*m/z*,

Table 3
Predicted ADMET data MTX (**1**) versus the most active compounds **29**, **33**, **59** and **61**.

Compound	BBB	HIA	AQ sol log S	CYP 2D6 substrate/inhibition	AMES toxicity	carcinogenicity
MTX (1)	0.9930	0.9088	−3	Non-substrate/noninhibitor	Nontoxic	Noncarcinogenic
29	0.9770	0.8492	−4	Non-substrate/noninhibitor	Nontoxic	Noncarcinogenic
33	0.9763	0.7401	−4	Non-substrate/noninhibitor	Nontoxic	Noncarcinogenic
59	0.9778	0.9491	−4	Non-substrate/noninhibitor	Nontoxic	Noncarcinogenic
61	0.9772	0.9474	−4	Non-substrate/noninhibitor	Nontoxic	Noncarcinogenic

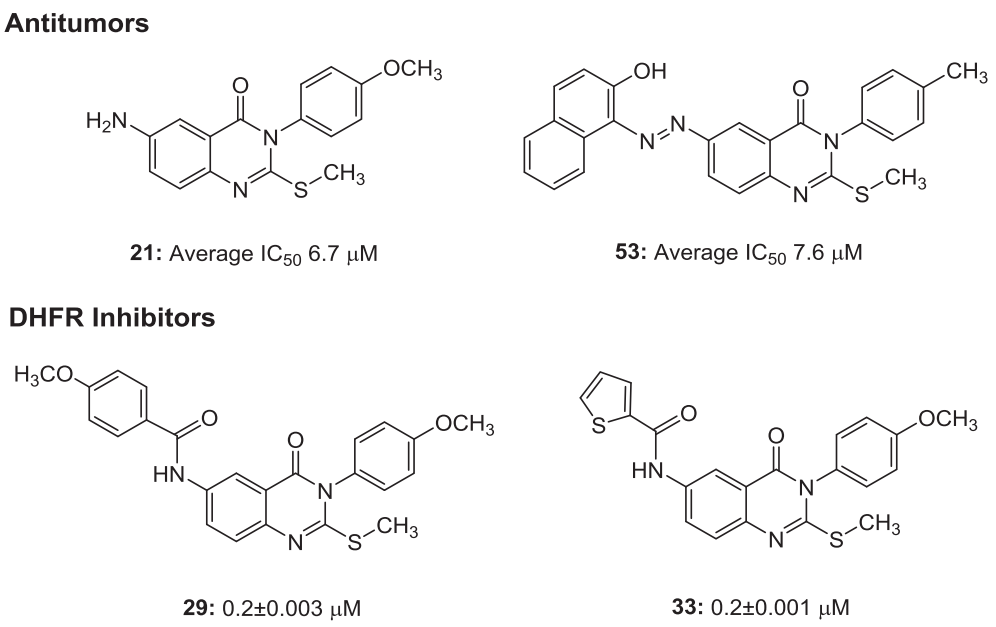

Fig. 10. Structures of the most active antitumors **21** and **53**, and the most active DHFR inhibitors **29**, **33**.

%) for $C_{16}H_{15}N_3O_2S$: (M^+ 313.1, 81.95), 90 (100).

*6.1.4. General procedure for the synthesis of 4-substituted-N-(3-(4-substituted-phenyl)-2-(methyl-thio)-4-oxo-3,4-dihydro-quinazolin-6-yl) benzamides (**25–30**)*

A mixture of 6-amino-quinazoline derivative (**20** or **21**, 0.005 mol) and the appropriate substituted benzoyl chloride (**22–24**, 0.007 mol) in pyridine (10 ml) was stirred at room temperature for 2 h. The reaction mixture was poured into ice and the formed precipitate was filtered, washed with water, dried and recrystallized from ethanol to give **25–30**.

*6.1.4.1. 4-Methyl-N-(2-(methyl-thio)-4-oxo-3-(4-methyl-phenyl)-3,4-dihydro-quinazolin-6-yl)benzamide (**25**)*. Off white powder (1.79 g, 86%), m.p. 280–3 °C. ^{1}H NMR (DMSO-d_6): δ 2.40 (s, 3H, CH_3Ph), 2.42 (s, 3H, CH_3Ph), 2.48(s, 3H, SCH_3), 7.31–7.37 (m, 6H, ArH), 7.64 (d, 1H, J = 8.4, ArH), 7.93 (d, 2H, J = 7.6 Hz, ArH), 8.26 (d, 1H, J = 8.4 Hz, ArH), 8.57 (s, 1H, ArH), 10.5 (s, 1H, NH), ^{13}C NMR: δ 15.5, 21.3, 21.5, 116.8, 120.0, 126.9, 127.9, 128.2, 129.5, 129.6, 130.4, 132.1, 133.9, 137.5, 139.9, 142.3, 144.0, 157.2, 161.2, 165.9. MS (*m/z*, %) for $C_{24}H_{21}N_3O_2S$: (M^+ 415.1, 100).

*6.1.4.2. 4-Methoxy-N-(2-(methyl-thio)-4-oxo-3-(4-methyl-phenyl)-3,4-dihydro-quinazolin-6-yl)benzamide (**26**)*. Greyish white powder (1.81 g, 84%), m.p. 281–3 °C. ^{1}H NMR (DMSO-d_6): δ 2.41 (s, 3H, CH_3Ph), 2.47 (s, 3H, SCH_3), 3.85(s, 3H, OCH_3), 7.09 (d, 2H, J = 8.0 Hz, ArH), 7.31–7.38 (m, 4H, ArH), 7.63 (d, 1H, J = 8.4 Hz, ArH), 8.01 (d, 2H, J = 8.4 Hz, ArH), 8.25 (d, 1H, J = 8.4 Hz, ArH), 8.55 (s, 1H, ArH), 10.45 (s, 1H, NH), ^{13}C NMR: δ 15.5, 21.3, 55.9, 114.2, 116.7, 120.0, 126.9, 127.0, 127.9, 129.6, 130.2, 130.4, 133.9, 137.6, 139.9, 143.9, 157.2, 161.2, 162.5, 165.5. MS (*m/z*, %) for $C_{24}H_{21}N_3O_3S$: (M^+ 431.2, 100).

*6.1.4.3. 4-Fluoro-N-[2-(methyl-thio)-4-oxo-3-(4-methyl-phenyl)-3,4-dihydro-quinazolin-6-yl]benzamide (**27**)*. White powder (1.7 g, 81%), m.p. 275–8 °C. ^{1}H NMR (DMSO-d_6): δ 2.41 (s, 3H, CH_3Ph), 2.47 (s, 3H, SCH_3), 7.32 (d, 2H, J = 8.4 Hz, ArH), 7.36–7.42 (m, 4H, ArH), 7.65 (d, 1H, J = 8.8, ArH), 8.07–8.11 (m, 2H, ArH), 8.23–8.26 (dd, 1H, J = 2.4, 8.8 Hz, ArH), 8.55 (d, 1H, J = 2.4 Hz, ArH), 10.61 (s, 1H, NH), ^{13}C NMR: δ 15.5, 21.3, 115.8, 116.0, 116.9, 120.0, 124.4, 127.0, 127.9, 129.6, 130.4, 130.9, 131.0, 131.4, 133.9, 137.3, 140.0, 144.1, 150.1, 157.4, 161.2, 163.5, 165.0. MS (*m/z*, %) for $C_{23}H_{18}FN_3O_2S$: (M^+ 419.0, 100).

*6.1.4.4. N-(3-(4-Methoxy-phenyl)-2-(methyl-thio)-4-oxo-3,4-dihydro-quinazolin-6-yl)-4-methyl-benzamide (**28**)*. Yellowish-white powder (1.88 g, 87%), m.p. 270–3 °C. ^{1}H NMR (DMSO-d_6): δ 2.40 (s, 3H, CH_3Ph), 2.47 (s, 3H, SCH_3), 3.85(s, 3H, OCH_3), 7.10 (d, 2H, J = 7.6 Hz, ArH), 7.35–7.37 (m, 4H, ArH), 7.63 (d, 1H, J = 8.4 Hz, ArH), 7.92 (d, 2H, J = 6.8 Hz, ArH), 8.25 (d, 1H, J = 8.4 Hz, ArH), 8.57 (s, 1H, ArH), 10.5 (s, 1H, NH), ^{13}C NMR: δ 15.5, 21.5, 55.9, 115.1, 116.8, 120.0, 126.9, 127.9, 128.2, 129.0, 129.5, 131.1, 132.1, 137.5, 142.4, 144.0, 157.7, 160.5, 161.4, 165.9. MS (*m/z*, %) for $C_{24}H_{21}N_3O_3S$: (M^+ 431.1, 31.21), 119 (100).

*6.1.4.5. 4-Methoxy-N-(3-(4-methoxy-phenyl)-2-(methyl-thio)-4-oxo-3,4-dihydro-quinazolin-6-yl)benzamide (**29**)*. Greyish white powder (1.97 g, 88%), m.p. 290–3 °C. ^{1}H NMR ($CDCl_3$): δ 2.54 (s, 3H, SCH_3), 3.86 (s, 3H, OCH_3), 3.90 (s, 3H, OCH_3), 6.98–7.03 (m, 4H, ArH), 7.22 (d, 2H, J = 8.8 Hz, ArH), 7.68 (d, 1H, J = 8.8 Hz, ArH), 7.88 (d, 2H, J = 8.8 Hz, ArH), 8.08 (d, 1H, J = 2.4 Hz, ArH), 8.27 (s, 1H, NH), 8.51–8.54 (dd, 1H, J = 2.4, 8.8 Hz, ArH), ^{13}C NMR: δ 15.6, 55.49, 55.50, 114.0, 114.9, 116.9, 119.9, 126.6, 127.2, 127.9, 128.3, 129.1, 130.2, 136.3, 144.6, 157.5, 160.6, 161.9, 162.6, 165.2. MS (*m/z*, %) for $C_{24}H_{21}N_3O_4S$: (M^+ 447.1, 94.93), 135 (100).

*6.1.4.6. 4-Fluoro-N-(3-(4-methoxy-phenyl)-2-(methyl-thio)-4-oxo-3,4-dihydro-quinazolin-6-yl)benzamide (**30**)*. White powder (1.79 g, 82%), m.p. 305–8 °C. ^{1}H NMR (DMSO-d_6): δ 2.47 (s, 3H, SCH_3), 3.84 (s, 3H, OCH_3), 7.10 (d, 2H, J = 8.8 Hz, ArH), 7.34–7.41 (m, 4H, ArH), 7.64 (d, 1H, J = 8.8, ArH), 8.06–8.10 (m, 2H, ArH), 8.21–8.23 (dd, 1H, J = 2, 8.8 Hz, ArH), 8.54 (d, 1H, J = 2.0 Hz, ArH), 10.61 (s, 1H, NH), ^{13}C NMR: δ 15.5, 55.9, 115.1, 115.8, 116.0, 117.0, 120.0, 127.0, 127.9, 128.9, 130.9, 131.0, 131.1, 131.39, 131.42, 137.2, 144.2, 157.8, 160.5, 161.4, 163.4, 165.1. MS (*m/z*, %) for $C_{23}H_{18}FN_3O_3S$: (M^+ 435, 100).

*6.1.5. General procedure for the synthesis of N-(3-(4-substituted-phenyl)-2-(methyl-thio)-4-oxo-3,4-dihydro-quinazolin-6-yl)thiophene-2-carboxamides (**32** and **33**)*

A mixture of 6-amino-quinazoline derivative (**20** or **21**, 0.005 mol) and thiophene-2-carbonyl chloride (**31**, 0.733 g, 0.007 mol) in pyridine (10 ml) was stirred at room temperature for 2 h. The reaction mixture

was poured into ice and the formed precipitate was filtered, washed with water, dried and recrystallized from ethanol to give **32** and **33**.

*6.1.5.1. N-(2-(Methyl-thio)-4-oxo-3-(4-methyl-phenyl)-3,4-dihydro-quinazolin-6-yl)thiophene-2-carboxamide (**32**)*. Off white powder (1.81 g, 89%), m.p. 225–8 °C. ^{1}H NMR (DMSO-d_6): δ 2.41 (s, 3H, CH_3Ph), 2.47 (s, 3H, SCH_3), 7.24–7.26 (dd, 1H, J = 3.6, 4.0 Hz, ArH), 7.31–7.38 (m, 4H, ArH), 7.65 (d, 1H, J = 8.8 Hz, ArH), 7.9 (d, 1H, J = 4.8 Hz, ArH), 8.09 (d, 1H, J = 3.2 Hz, ArH), 8.23–8.26 (dd, 1H, J = 2.4, 8.8 Hz, ArH), 8.49 (d, 1H, J = 2.4 Hz, ArH), 10.57 (s, 1H, NH), ^{13}C NMR: δ 15.6, 21.3, 116.8, 120.1, 124.4, 127.1, 127.8, 128.7, 129.6, 130.4, 132.8, 133.9, 137.0, 140.1, 144.1, 150.1, 157.4, 160.5, 161.2. MS (*m/z*, %) for $C_{21}H_{17}N_3O_2S_2$: (M^+ 407.2, 100).

*6.1.5.2. N-(3-(4-Methoxy-phenyl)-2-(methyl-thio)-4-oxo-3,4-dihydro-quinazolin-6-yl)thiophene-2-carboxamide (**33**)*. Yellowish-white powder (1.9 g, 90%), m.p. 190–3 °C. ^{1}H NMR (DMSO-d_6): δ 2.47 (s, 3H, SCH_3), 3.85 (s, 3H, OCH_3), 7.10 (d, 2H, J = 8.8 Hz, ArH), 7.24–7.27 (dd, 1H, J = 3.6, 4.0 Hz, ArH), 7.37 (d, 2H, J = 8.8 Hz, ArH), 7.64 (d, 1H, J = 8.8 Hz, ArH), 7.89–7.91 (dd, 1H, J = 1.2, 4.8 Hz, ArH), 8.08–8.09 (dd, 1H, J = 1.2, 4.0 Hz, ArH), 8.22–8.25 (dd, 1H, J = 2.4, 8.8 Hz, ArH), 8.48 (d, 1H, J = 2.4 Hz, ArH), 10.56 (s, 1H, NH), ^{13}C NMR: δ 15.5, 55.9, 115.1, 116.8, 120.1, 125.5, 127.1, 127.7, 128.7, 128.9, 129.9, 131.1, 132.8, 137.0, 140.1, 144.1, 157.8, 160.5, 161.3. MS (*m/z*, %) for $C_{21}H_{17}N_3O_3S_2$: (M^+ 423.0, 100).

*6.1.6. General procedure for the synthesis of N-(3-(4-substituted-phenyl)-2-(methyl-thio)-4-oxo-3,4-dihydro-quinazolin-6-yl)- derivatives of acetic, propionic or butyric acid amides (**37–42**)*

A mixture of 6-amino-quinazoline derivative (**20** or **21**, 0.005 mol), the appropriate acid chloride (**34–36**, 0.007 mol) and TEA (0.5 ml) in methylene chloride (20 ml) was stirred at room temperature for 2 h. Then the reaction mixture was evaporated under vacuum and the separated solid was washed with water, dried and recrystallized from ethanol to give **37–42**.

*6.1.6.1. N-(2-(Methyl-thio)-4-oxo-3-(4-methyl-phenyl)-3,4-dihydro-quinazolin-6-yl)acetamide (**37**)*. Greyish-white powder (1.31 g, 77%), m.p. 250–2 °C. ^{1}H NMR ($CDCl_3$): δ 1.84 (s, 3H, $COCH_3$), 2.47 (s, 3H, CH_3Ph), 2.53 (s, 3H, SCH_3), 7.22 (d, 2H, J = 8.0, ArH), 7.37 (d, 2H, J = 8.0 Hz, ArH), 7.65 (d, 1H, J = 8.8 Hz, ArH), 8.03 (d, 1H, J = 2.4 Hz, ArH), 8.42 (s, 1H, NH), 8.52–8.55 (dd, 1H, J = 2.4, 8.8 Hz, ArH). ^{13}C NMR: δ 15.6, 21.4, 24.0, 115.9, 119.7, 127.2, 127.6, 128.9, 130.5, 133.4, 136.7, 140.4, 144.4, 156.8, 162.0, 169.1. MS (*m/z*, %) for $C_{18}H_{17}N_3O_2S$: (M^+ 339.1, 100).

*6.1.6.2. N-(2-(Methyl-thio)-4-oxo-3-(4-methyl-phenyl)-3,4-dihydro-quinazolin-6-yl)propion-amide (**38**)*. Yellowish-white powder (1.33 g, 75%), m.p. 240–2 °C. ^{1}H NMR ($CDCl_3$): δ 1.18 (t, 3H, J = 7.2 Hz, CH_3), 2.16 (q, 2H, J = 7.6 Hz, $COCH_2$), 2.48 (s, 3H, CH_3Ph), 2.53 (s, 3H, SCH_3), 7.22 (d, 2H, J = 8.0 Hz, ArH), 7.38 (d, 2H, J = 8.0 Hz, ArH), 7.65 (d, 1H, J = 9.2 Hz, ArH), 8.00 (d, 1H, J = 2.8 Hz, ArH), 8.07 (s, 1H, NH), 8.5–8.53 (dd, 1H, J = 2.8, 9.2 Hz, ArH), ^{13}C NMR: δ 9.6, 15.6, 21.5, 30.2, 115.9, 119.8, 127.2, 127.6, 128.9, 130.4, 133.4, 136.5, 140.3, 144.4, 156.9, 161.9, 172.5. MS (*m/z*, %) for $C_{19}H_{19}N_3O_2S$: (M^+ 353.0, 28.79), 68 (100).

*6.1.6.3. N-(2-(Methyl-thio)-4-oxo-3-(4-methyl-phenyl)-3,4-dihydro-quinazolin-6-yl)butyramide (**39**)*. Off-white powder (1.52 g, 83%), m.p. 214–6 °C. ^{1}H NMR ($CDCl_3$): δ 0.98 (t, 3H, J = 7.2 Hz, CH_3), 1.66–1.73 (m, 2H, CH_2), 2.13 (t, 2H, J = 7.2 Hz, $COCH_2$), 2.48 (s, 3H, CH_3Ph), 2.53 (s, 3H, SCH_3), 7.22 (d, 2H, J = 8.0 Hz, ArH), 7.37 (d, 2H, J = 8.0 Hz, ArH), 7.64 (d, 1H, J = 8.8 Hz, ArH), 8.01 (d, 1H, J = 2.4 Hz, ArH), 8.08 (s, 1H, NH), 8.47–8.5 (dd, 1H, J = 2.4, 8.8 Hz, ArH), ^{13}C NMR: δ 13.7, 15.6, 18.9, 21.4, 39.0, 116.1, 119.8, 127.2, 127.7, 128.8, 130.4, 133.4, 136.4, 140.3, 144.4, 156.9, 161.9, 171.8. MS (*m/z*, %) for $C_{20}H_{21}N_3O_2S$: (M^+ 367.0, 98.91), 182 (1 0 0).

*6.1.6.4. N-(3-(4-Methoxy-phenyl)-2-(methyl-thio)-4-oxo-3,4-dihydro-quinazolin-6-yl)acetamide (**40**)*. Off-white powder (1.44 g, 81%), m.p. 310–2 °C. ^{1}H NMR (DMSO-d_6): δ 2.09 (s, 3H, $COCH_3$), 2.45 (s, 3H, SCH_3), 3.84 (s, 3H, OCH_3), 7.09 (d, 2H, J = 8.8 Hz, ArH), 7.35 (d, 2H, J = 8.8 Hz, ArH), 7.58 (d, 1H, J = 8.8 Hz, ArH), 7.97–8 (dd, 1H, J = 2.4, 8.8 Hz, ArH), 8.36 (d, 1H, J = 2.4 Hz, ArH), 10.29 (s, 1H, NH), , ^{13}C NMR: δ 15.5, 24.5, 55.9, 115.0, 115.3, 120.1, 126.7, 127.1, 128.9, 131.1, 137.5, 143.7, 157.4, 160.4, 161.3, 169.0. MS (*m/z*, %) for $C_{18}H_{17}N_3O_3S$: (M^+ 355.1, 100).

*6.1.6.5. N-(3-(4-Methoxy-phenyl)-2-(methyl-thio)-4-oxo-3,4-dihydro-quinazolin-6-yl)propion-amide (**41**)*. Yellowish-white powder (1.44 g, 78%), m.p. 275–8 °C. ^{1}H NMR (DMSO-d_6): δ 1.10 (t, 3H, J = 7.6 Hz, CH_3), 2.36 (q, 2H, J = 7.6 Hz, $COCH_2$), 2.45 (s, 3H, SCH_3), 3.84 (s, 3H, OCH_3), 7.09 (d, 2H, J = 8.4 Hz, ArH), 7.35 (d, 2H, J = 8.4 Hz, ArH), 7.58 (d, 1H, J = 8.8 Hz, ArH), 7.99–8.02 (dd, 1H, J = 2.0, 8.8 Hz, ArH), 8.38 (d, 1H, J = 2.0 Hz, ArH), 10.21 (s, 1H, NH), ^{13}C NMR: δ 10.0, 15.5, 30.0, 55.9, 115.0, 115.4, 120.1, 126.7, 127.1, 129.0, 131.1, 137.6, 143.6, 157.3, 160.4, 161.3, 172.7. MS (*m/z*, %) for $C_{19}H_{19}N_3O_3S$: (M^+ 369.1, 100).

*6.1.6.6. N-(3-(4-Methoxy-phenyl)-2-(methyl-thio)-4-oxo-3,4-dihydro-quinazolin-6-yl)butyr-amide (**42**)*. Greyish-white powder (1.53 g, 80%), m.p. 292–5 °C. ^{1}H NMR ($CDCl_3$): δ 0.98 (t, 3H, J = 7.6 Hz, CH_3), 1.68–1.77 (m, 2H, CH_2), 2.25 (t, 2H, J = 7.6 Hz, $COCH_2$), 2.51 (s, 3H, SCH_3), 3.87 (s, 3H, OCH_3), 7.04 (d, 2H, J = 8.8 Hz, ArH), 7.22 (d, 2H, J = 8.8 Hz, ArH), 7.61 (d, 1H, J = 9.2 Hz, ArH), 8.00 (d, 1H, J = 2.8 Hz, ArH), 8.44–8.46 (dd, 1H, J = 2.8, 9.2 Hz, ArH), 8.59 (s, 1H, NH), ^{13}C NMR: δ 13.8, 15.6, 19.0, 39.2, 55.5, 114.9, 116.1, 119.8, 127.0, 127.5, 128.4, 130.2, 136.7, 144.3, 157.1, 160.6, 162.0, 172.0. MS (*m/z*, %) for $C_{20}H_{21}N_3O_3S$: (M^+ 384.0, 100).

*6.1.7. General procedure for the synthesis of 6-[(4-hydroxy-3-substituted-phenyl)diazenyl]-3-(4-substituted-phenyl)-2-(methyl-thio)quinazolin-4(3H)-ones (**45–48**)*

A stirred solution of 6-amino-quinazoline derivative (**20** or **21**, 0.005 mol) in 4.0 ml of conc. HCl was cooled in an ice-bath to 0–5 °C and diazotized with a solution of 0.4 g $NaNO_2$ (0.005 mol) in 2 ml H_2O. The cold diazonium solution was added slowly to a well stirred solution of phenol or *o*-cresol (**43** or **44**, 0.005 mol) in 2.5 M NaOH (10 ml) at 0–5 °C. The reaction mixture was stirred for another 2 h. The crude product was filtered, washed with cold dil. HCl, dried and recrystallized from ethanol to give **45–48**.

*6.1.7.1. 6-[(4-Hydroxy-phenyl)diazenyl]-2-(methyl-thio)-3-(4-methyl-phenyl)quinazolin-4(3H)-one (**45**)*. Dark yellow crystals (1.39 g, 69%), m.p. 275–8 °C. ^{1}H NMR (DMSO-d_6): δ 2.42 (s, 3H, CH_3Ph), 2.51 (s, 3H, SCH_3), 6.97 (d, 2H, J = 8.4 Hz, ArH), 7.35–7.38 (m, 4H, ArH), 7.76 (d, 1H, J = 8.4 Hz, ArH), 7.86 (d, 2H, J = 8.4 Hz, ArH), 8.26 (d, 1H, J = 8.4 Hz, ArH), 8.44 (s, 1H, ArH), 10.43 (s, 1H, OH). ^{13}C NMR: δ 15.7, 20.4, 56.0, 115.2, 118.6, 120.6, 121.9, 123.3, 127.7, 127.9, 128.7, 129.1, 131, 135.4, 138.7, 149.2, 150.5, 153.4, 160.6, 161.2, 161.3. MS (*m/z*, %) for $C_{26}H_{20}N_4O_2S$: (M^+ 402.1, 100).

*6.1.7.2. 6-[(4-Hydroxy-phenyl)diazenyl]-3-(4-methoxy-phenyl)-2-(methyl-thio)quinazolin-4(3H)-one (**46**)*. Dark orange crystals (1.29 g, 62%), m.p. 276–8 °C. ^{1}H NMR (DMSO-d_6): δ 2.51 (s, 3H, SCH_3), 3.85 (s, 3H, OCH_3), 6.97 (d, 2H, J = 8.8 Hz, ArH), 7.12 (d, 2H, J = 8.8 Hz, ArH), 7.41 (d, 2H, J = 8.8 Hz, ArH), 7.75 (d, 1H, J = 8.8 Hz, ArH), 7.86 (d, 2H, J = 8.8 Hz, ArH), 8.24–8.27 (dd, ^{1}H, J = 2.0, 8.8 Hz, ArH), 8.44 (d, 1H, J = 2.0 Hz, ArH), 10.45 (s, 1H, OH). ^{13}C NMR: δ 15.7, 56.0, 115.1, 116.5, 120.5, 122.0, 125.6, 127.6, 127.9, 128.7, 131.0, 145.7, 149.1, 149.5, 160.6, 160.9, 161.4, 161.8. MS (*m/z*, %) for $C_{26}H_{20}N_4O_3S$: (M^+ 418.1, 100).

*6.1.7.3. 6-[(4-Hydroxy-3-methyl-phenyl)diazenyl]-2-(methyl-thio)-3-(4-methyl-phenyl)quina-zolin-4(3H)-one (**47**)*. Orange crystals (1.19 g, 57%), m.p. 212–5 °C. ^{1}H NMR (DMSO-d_6): δ 2.23 (s, 3H, CH_3Ph), 2.42 (s, 3H, CH_3Ph), 2.52 (s, 3H, SCH_3), 6.98 (d, 1H, J = 8.8 Hz, ArH), 7.36–7.40 (m, 4H, ArH), 7.70–7.73 (dd, 1H, J = 2.4, 8.4 Hz, ArH), 7.75–7.78 (m, 2H, ArH), 8.24–8.27 (dd, 1H, J = 2.4, 8.8 Hz, ArH), 8.44 (d, 1H, J = 2.4 Hz, ArH), 10.38 (s, 1H, OH). ^{13}C NMR: δ 15.6, 16.5, 21.3, 115.5, 120.5, 121.8, 124.1, 125.3, 125.7, 127.6, 127.9, 129.5, 130.5, 133.8, 140.1, 145.5, 149, 149.7, 160, 160.4, 161.2. MS (*m/z*, %) for $C_{23}H_{20}N_4O_2S$: (M^+ 416.1, 100).

*6.1.7.4. 6-[(4-Hydroxy-3-methyl-phenyl)diazenyl]-3-(4-methoxy-phenyl)-2-(methyl-thio)quina-zolin-4(3H)-one (**48**)*. Brown crystals (1.17 g, 54%), m.p. 265–8 °C. ^{1}H NMR (DMSO-d_6): δ 2.23 (s, 3H, CH_3Ph), 2.51 (s, 3H, SCH_3), 3.86 (s, 3H, OCH_3), 6.99 (d, 1H, J = 8.8 Hz, ArH), 7.12 (d, 2H, J = 8.8 Hz, ArH), 7.41 (d, 2H, J = 8.8 Hz, ArH), 7.70–7.73 (dd, 1H, J = 2.0, 8.8 Hz, ArH), 7.75 (d, 1H, J = 8.8 Hz, ArH), 7.76 (s, 1H, ArH), 8.23–8.26 (dd, 1H, J = 2.0, 8.8 Hz, ArH), 8.43 (d, 1H, J = 2.0 Hz, ArH), 10.4 (s, 1H, OH). ^{13}C NMR: δ 15.7, 16.5, 56.0, 115.1, 115.5, 120.6, 121.8, 124.0, 125.3, 125.6, 127.6, 127.9, 128.7, 131.0, 145.5, 149.0, 149.6, 160.0, 160.6, 160.8, 161.4. MS (*m/z*, %) for $C_{23}H_{20}N_4O_3S$: (M^+ 432.1, 100).

*6.1.8. General procedure for the synthesis of 6-[(2-hydroxy-5-methyl-phenyl)diazenyl)]-3-(4-substituted-phenyl)-2-(methyl-thio)quinazolin-4(3H)-ones (**50** and **51**)*

A stirred solution of 6-amino-quinazoline derivative (**20** or **21**, 0.005 mol) in 4.0 ml of conc. HCl was cooled in an ice-bath to 0–5 °C and diazotized with the solution of 0.4 g $NaNO_2$ (0.005 mol) in 2 ml H_2O. The cold diazonium solution was added slowly to a well stirred solution of *p*-cresol (**49**, 0.54 g, 0.005 mol) in 2.5 M NaOH (10 ml) at 0–5 °C. The reaction mixture was stirred for another 2 h. The crude product was filtered, washed with cold dil. HCl, dried and recrystallized from ethanol to give **50** and **51**.

*6.1.8.1. 6-[(2-Hydroxy-5-methyl-phenyl)diazenyl]-2-(methyl-thio)-3-(4-methyl-phenyl)quina-zolin-4(3H)-one (**50**)*. Dark brown crystals (1.02 g, 49%), m.p. 208–10 °C. ^{1}H NMR (DMSO-d_6): δ 2.30 (s, 3H, CH_3Ph), 2.43 (s, 3H, CH_3Ph), 2.53 (s, 3H, SCH_3), 6.99 (d, 1H, J = 8.4 Hz, ArH), 7.25–7.28 (dd, 1H, J = 2.0, 8.4 Hz, ArH), 7.36–7.41 (m, 4H, ArH), 7.60 (d, 1H, J = 2.0 Hz, ArH), 7.77 (d, 1H, J = 8.8 Hz, ArH), 8.45–8.48 (dd, 1H, J = 2.4, 8.8 Hz, ArH), 8.6 (d, 1H, J = 2.4 Hz, ArH), 10.8 (s, 1H, OH). ^{13}C NMR: δ 15.7, 20.4, 21.3, 118.6, 120.6, 121.9, 123.2, 127.7, 127.9, 129.1, 129.5, 130.5, 133.7, 135.2, 138.7, 140.1, 149.2, 149.5, 153.4, 160.8, 161.2. MS (*m/z*, %) for $C_{22}H_{18}N_4O_2S$: (M^+ 416.1, 100).

*6.1.8.2. 6-[(2-Hydroxy-5-methyl-phenyl)diazenyl]-3-(4-methoxy-phenyl)-2-(methyl-thio)quina-zolin-4(3H)-one (**51**)*. Dark orange crystals (1.1 g, 51%), m.p. 229–32 °C. ^{1}H NMR (DMSO-d_6): δ 2.30 (s, 3H, CH_3Ph), 2.52 (s, 3H, SCH_3), 3.86 (s, 3H, OCH_3), 6.99 (d, 1H, J = 8.4 Hz, ArH), 7.12 (d, 2H, J = 8.8 Hz, ArH), 7.25–7.28 (dd, 1H, J = 2.0, 8.4 Hz, ArH), 7.42 (d, 2H, J = 8.8 Hz, ArH), 7.60 (s, 1H, ArH), 7.77 (d, 1H, J = 8.8 Hz, ArH), 8.45–8.47 (dd, 1H, J = 2.4, 8.8 Hz, ArH), 8.60 (d, 1H, J = 2.0 Hz, ArH), 10.8 (s, 1H, OH). ^{13}C NMR: δ 15.7, 20.4, 56.0, 115.2, 118.6, 120.6, 121.9, 123.3, 127.7, 127.9, 128.7, 129.1, 131.0, 135.4, 138.7, 149.2, 150.5, 153.4, 160.6, 161.2, 161.3. MS (*m/z*, %) for $C_{23}H_{20}N_4O_2S$: (M^+ 432, 100).

*6.1.9. General procedure for the synthesis of 6-[(2-hydroxy-naphthalen-1-yl)diazenyl]-3-(4-substituted-phenyl)-2-(methyl-thio)quinazolin-4(3H)-one (**53** and **54**)*

A stirred solution of 6-amino-quinazoline derivative (**20** or **21**, 0.005 mol) in 4.0 ml of conc. HCl was cooled in an ice-bath to 0–5 °C and diazotized with the solution of 0.4 g $NaNO_2$ (0.005 mol) in 2 ml H_2O. The cold diazonium solution was added slowly to a stirred solution of naphthalen-2-ol (**52**, 0.72 g, 0.005 mol) in 2.5 M NaOH (10 ml) at 0–5 °C. The reaction mixture was stirred for another 2 h. The crude product was filtered, washed with cold dil. HCl, dried and recrystallized from ethanol to give **53** and **54**.

*6.1.9.1. 6-[(2-Hydroxy-naphthalen-1-yl)diazenyl]-2-(methyl-thio)-3-(4-methyl-phenyl)quina-zolin-4(3H)-one (**53**)*. Dark red crystals (1.2 g, 53%), m.p. 286–9 °C.. ^{1}H NMR ($CDCl_3$): δ 2.50 (s, 3H, CH_3Ph), 2.58 (s, 3H, SCH_3), 6.94 (d, 1H, J = 9.2 Hz, ArH), 7.26 (d, 2H, J = 8.4 Hz, ArH), 7.4 (d, 2H, J = 8.0, ArH), 7.45 (d, 1H, J = 6.8 Hz, ArH), 7.59 (t, 1H, J = 6.8 Hz, ArH), 7.65 (d, 1H, J = 7.6 Hz, ArH), 7.77 (d, 2H, J = 9.2 Hz, ArH), 8.21–8.24 (dd, 1H, J = 2.4, 9.2 Hz, ArH), 8.55 (d, 1H, J = 2.4 Hz, ArH), 8.65 (d, 1H, J = 8.0 Hz, ArH), 16.15 (s, 1H, OH). ^{13}C NMR: δ 15.6, 21.5, 117.7, 120.7, 122.0, 124.1, 124.6, 125.9, 128.0, 128.2, 128.6, 128.7, 129.0, 130.4, 130.5, 133.1, 133.4, 139.9, 140.4, 143.1, 147.3, 158.8, 161.6, 169.8. MS (*m/z*, %) for $C_{22}H_{18}N_4O_3S$: (M^+ 452.1, 100).

*6.1.9.2. 6-[(2-Hydroxy-naphthalen-1-yl)diazenyl]-3-(4-methoxy-phenyl)-2-(methyl-thio)quina-zolin-4(3H)-one (**54**)*. Dark red crystals (1.29 g, 55%), m.p. 309–12 °C. ^{1}H NMR ($CDCl_3$): δ 2.58 (s, 3H, SCH_3), 3.92 (s, 3H, OCH_3), 6.95 (d, 1H, J = 9.2 Hz, ArH), 7.10 (d, 2H, J = 8.8 Hz, ArH), 7.29 (d, 2H, J = 8.8, ArH), 7.44 (t, 1H, J = 7.6 Hz, ArH), 7.59 (t, 1H, J = 7.2 Hz, ArH), 7.66 (d, 1H, J = 8.0 Hz, ArH), 7.76–7.79 (m, 2H, ArH), 8.21–8.24 (dd, 1H, J = 2.4, 9.2 Hz, ArH), 8.55 (d, 1H, J = 2.4 Hz, ArH), 8.66 (d, 1H, J = 8.0 Hz, ArH), 16.15 (s, 1H, OH). ^{13}C NMR: δ 15.7, 55.6, 115.0, 117.7, 120.7, 122.0, 124.1, 124.6, 125.9, 127.9, 128.17, 128.22, 128.7, 129.0, 130.2, 130.4, 133.4, 139.9, 143.1, 147.1, 159.2, 160.7, 161.7, 169.9. MS (*m/z*, %) for $C_{23}H_{20}N_4O_3S$: (M^+ 468.1, 100).

*6.1.10. General procedure for the synthesis of 1-(4-substituted-phenyl)-3-(3-(4-substituted-phenyl)-2-(methyl-thio)-4-oxo-3,4-dihydro-quinazolin-6-yl)thioureas (**56–61**)*

A solution of the 6-aminoquinazoline derivative (**20** or **21**, 0.005 mol), and the appropriate substituted phenylisothiocyanate derivative (**14**, **15** or **55**, 0.005 mol) in pyridine (10 ml) was stirred at room temperature for 6 h. Then the reaction mixture was poured into cold dil. HCl. The formed precipitate was filtered, washed with water, dried and recrystallized from ethanol to give (**56–61**).

*6.1.10.1. 1-(2-(Methyl-thio)-4-oxo-3-(4-methyl-phenyl)-3,4-dihydro-quinazolin-6-yl)-3-(4-methyl-phenyl)thiourea (**56**)*. Yellowish-white crystals (1.83 g, 82%), m.p. 108–10 °C. ^{1}H NMR ($CDCl_3$): δ 2.40 (s, 3H, CH_3Ph), 2.42 (s, 3H, CH_3Ph), 2.53 (s, 3H, SCH_3), 7.18 (d, 2H, J = 8.4 Hz, ArH), 7.23–7.28 (m, 4H, ArH), 7.33 (d, 2H, J = 8.0 Hz, ArH), 7.66 (d, 1H, J = 8.4 Hz, ArH), 8.0 (d, 1H, J = 2.0 Hz, ArH), 8.05 (s, 1H, NH), 8.08 (s, 1H, NH), 8.18–8.21 (dd, 1H, J = 2.0, 8.4 Hz, ArH). ^{13}C NMR: δ 15.6, 21.1, 21.4, 119.9, 121.7, 125.6, 125.9, 127.0, 128.7, 130.1, 130.4, 130.5, 132.5, 133.1, 135.8, 140.4, 146.1, 158.3, 161.6, 180.5. MS (*m/z*, %) for $C_{24}H_{22}N_4OS_2$: (M^+ 446.0, 23.62), 444 (100).

*6.1.10.2. 1-(4-Methoxy-phenyl)-3-(2-(methyl-thio)-4-oxo-3-(4-methyl-phenyl)-3,4-dihydro-quinazolin-6-yl)thiourea (**57**)*. Off-white crystals (1.97 g, 85%), m.p. 164–6 °C. ^{1}H NMR ($CDCl_3$): δ 2.46 (s, 3H, CH_3Ph), 2.54 (s, 3H, SCH_3), 3.86 (s, 3H, OCH_3), 6.99 (d, 2H, J = 8.8 Hz, ArH), 7.19 (d, 2H, J = 8.4 Hz, ArH), 7.29–7.36 (m, 4H, ArH), 7.67 (d, 1H, J = 8.0 Hz, ArH), 7.81 (s, 1H, NH), 7.82 (s, 1H, NH), 7.99 (s, 1H, ArH), 8.15 (d, 1H, J = 8.0 Hz, ArH). ^{13}C NMR: δ 15.6, 21.4, 55.6, 115.3, 120.0, 122.0, 124.0, 128.0, 128.1, 128.7, 130.5, 132.4, 132.5, 133.1, 135.6, 140.4, 146.3, 158.5, 161.5, 180.9. MS (*m/z*, %) for $C_{24}H_{22}N_4O_2S_2$: (M^+ 462.0, 2.87), 428 (100).

*6.1.10.3. 1-(4-Chloro-phenyl)-3-(2-(methyl-thio)-4-oxo-3-(4-methyl-phenyl)-3,4-dihydro-quinazolin-6-yl)thiourea (**58**)*. Pale yellow crystals (2.07 g, 89%), m.p. 129–32 °C. ^{1}H NMR ($CDCl_3$): δ 2.32 (s, 3H, CH_3Ph), 2.53 (s, 3H, SCH_3), 7.17 (d, 2H, J = 8.4 Hz, ArH), 7.23–7.37 (m, 6H,

ArH), 7.67 (d, 1H, J = 8.8 Hz, ArH), 8.03 (d, 1H, J = 2.4 Hz, ArH), 8.32–8.34 (dd, 1H, J = 2.4, 8.8 Hz, ArH), 8.38 (s, 1H, NH), 8.95 (s, 1H, NH). ^{13}C NMR: δ 15.7, 21.3, 119.4, 120.7, 126.5, 126.7, 127.0, 128.4, 129.0, 129.6, 130.6, 132.8, 133.1, 136.4, 140.7, 146.0, 158.0, 162.4, 180.7. MS (m/z, %) for $C_{23}H_{19}ClN_4OS_2$: (M + 2 467.1, 33.50), (M^+ 465.0, 12.31), 89 (100).

*6.1.10.4. 1-(3-(4-Methoxy-phenyl)-2-(methyl-thio)-4-oxo-3,4-dihydro-quinazolin-6-yl)-3-(4-methyl-phenyl)thiourea (**59**).* Off-white crystals (1.85 g, 80%), m.p. 136–8 °C. ^{1}H NMR ($CDCl_3$): δ 2.40 (s, 3H, CH_3Ph), 2.53 (s, 3H, SCH_3), 3.86 (s, 3H, OCH_3), 7.03 (d, 2H, J = 8.8 Hz, ArH), 7.21–7.26 (m, 6H, ArH), 7.66 (d, 1H, J = 8.4 Hz, ArH), 7.91 (s, 1H, NH), 7.95 (s, 1H, NH), 7.99 (d, 1H, J = 2.4 Hz, ArH), 8.16–8.19 (dd, 1H, J = 2.4, 8.4 Hz, ArH), ^{13}C NMR: δ 15.6, 21.1, 55.5, 115.0, 119.9, 121.8, 125.5, 125.9, 127.0, 128.1, 130.1, 130.6, 132.4, 135.7, 137.9, 146.1, 158.8, 160.6, 161.7, 180.5. MS (m/z, %) for $C_{24}H_{22}N_4O_2S_2$: (M^+ 462.0, 12.98), 460 (100).

*6.1.10.5. 1-(4-Methoxy-phenyl)-3-(3-(4-methoxy-phenyl)-2-(methyl-thio)-4-oxo-3,4-dihydro-quinazolin-6-yl)thiourea (**60**).* Yellowish white crystals (1.96 g, 82%), m.p. 168–70 °C. ^{1}H NMR ($CDCl_3$): δ 2.53 (s, 3H, SCH_3), 3.86 (s, 3H, OCH_3), 3.87 (s, 3H, OCH_3), 6.99 (d, 2H, J = 8.8 Hz, ArH), 7.03 (d, 2H, J = 8.8 Hz, ArH), 7.21 (d, 2H, J = 8.8 Hz, ArH), 7.29 (d, 2H, J = 8.8 Hz, ArH), 7.66 (d, 1H, J = 8.8 Hz, ArH), 7.84 (s, 1H, NH), 7.85 (s, 1H, NH), 7.99 (d, 1H, J = 2.0 Hz, ArH), 8.16–8.19 (dd, 1H, J = 2.0, 8.8 Hz, ArH), ^{13}C NMR: δ 15.7, 55.5, 55.6, 115.0, 115.2, 119.9, 121.8, 127.0, 128.0, 128.1, 130.0, 130.1, 132.4, 135.7, 146.1, 158.8, 159.2, 160.6, 161.7, 180.9. MS (m/z, %) for $C_{24}H_{22}N_4O_3S_2$: (M^+ 462.0, 12.98), 460 (100).

*6.1.10.6. 1-(4-Chloro-phenyl)-3-(3-(4-methoxy-phenyl)-2-(methyl-thio)-4-oxo-3,4-dihydro-quinazolin-6-yl)thiourea (**61**).* Pale yellow crystals (2.13 g, 88%), m.p. 143–6 °C. ^{1}H NMR ($CDCl_3$): δ 2.53 (s, 3H, SCH_3), 3.77 (s, 3H, OCH_3), 6.92 (d, 2H, J = 8.8 Hz, ArH), 7.20 (d, 2H, J = 8.8 Hz, ArH), 7.25 (d, 2H, J = 8.4 Hz, ArH), 7.34 (d, 2H, J = 8.4 Hz, ArH), 7.68 (d, 1H, J = 8.8 Hz, ArH), 8.03 (d, 1H, J = 2.4 Hz, ArH), 8.24 (s, 1H, NH), 8.31 (d, 1H, J = 8.8 Hz, ArH), 8.75 (s, 1H, NH), ^{13}C NMR: δ 15.7, 55.4, 115.0, 119.4, 120.8, 126.8, 127.1, 127.7, 129.1, 129.8, 130.0, 132.0, 133.1, 136.2, 146.1, 158.6, 160.7, 162.5, 180.7. MS (m/z, %) for $C_{23}H_{19}ClN_4O_2S_2$: (M + 2 483.1, 13.47), (M^+ 481.0, 6.75), 480 (100).

6.2. Biological evaluation

6.2.1. Antitumor screening

6.2.1.1. In vitro antitumor evaluation. Four human tumor cell lines namely; mammary gland breast cancer (MCF-7), colorectal carcinoma (HCT-116), human prostate cancer (PC-3) and epitheliod Carcinoma (Hela) were used in the antitumor activity evaluation assay. MTT assay was used to determine the inhibitory effects of compounds on cell growth of the cell lines mentioned above. This colorimetric assay is based on mitochondrial succinate dehydrogenase conversion of the yellow tetrazolium bromide (MTT) to a purple formazan derivative by in viable cells. Cell lines were cultured in RPMI-1640 medium with 10% fetal bovine serum. Antibiotics added were 100 units/ml penicillin and 100 µg/ml streptomycin at 37 °C in a 5% CO_2 incubator. The cell lines were seeded in a 96-well plate at a density of 1.0x10^4 cells/well at 37 °C for 48 h under 5% CO_2. After incubation the cells were treated with different concentration of tested compounds and incubated for 72 h. After 72 h of drug treatment, 20 µl of MTT solution at 5 mg/ml was added and incubated for 4 h. After that, 100 µl dimethyl sulfoxide (DMSO) were added into each well to dissolve the purple formazan formed. The colorimetric assay is measured and recorded at absorbance of 570 nm using a plate reader (EXL 800, USA). The relative cell viability in percentage was calculated as (A570 of treated samples/A570 of untreated sample) X 100 (Table 1), [32–34].

*6.2.1.2. Cytotoxicity MTT assay for compounds **59** and **61**.* Tumor cell Lines were acquired from American Type Culture Collection, cells were cultured using Dulbecco's Modified Eagle Medium (DMEM) (Invitrogen/Life Technologies) augmented with 10% fetal bovine serum (Hyclone), 10 µg/ml of insulin (Sigma), and 1% penicillin-streptomycin. All of the other reagents and chemicals were obtained from Sigma chemical company. The cells (Hela and HCT-116) were subcultured into a 96-well plate with 1 × 10^4 cells per well in medium, at 37 °C, 5% CO_2 and 95% air atmosphere, before being treated with or without differenet concentrations of test compounds **59** and **61**, each in triplicate for 24 h. At the end of the incubation, the cells were harvested and washed with phosphate buffered saline (PBS). 20 µl of MTT was added to each well and incubated for 2 h before 200 µl DMSO was added. The absorbance was measured on an ELISA reader (Multiskan EX, Labsystems) at a test wavelength of 570 nm [36].

6.2.1.3. Flow cytometry analysis of DNA content for cell cycle and apoptosis. Hela and HCT-116 cell lines (each 2 × 10^5 cells/well) each in 12-well plates were incubated with different concentrations of test compounds **59 (**for Hela cell line**)** and **61** (for HCT-116 cell line) for various time-periods before the cells were harvested. The cells were fixed gently in 70% ethanol (in PBS) in ice overnight and were then suspended in PBS containing 40 µg/ml PI, 0.1 mg/ml RNase A (Sigma, USA) and 0.1% triton x-100. After 30 min at 37 °C in the dark, the cells were analyzed by flow cytometry (Becton Dickinson, San Jose, CA, USA) equipped with an argon laser at 488 nm. Then cell cycle and apoptosis were determined and examined [58–60].

6.2.2. Dihydrofolate reductase (DHFR) inhibition assay

The assay mixture contained 50 µM Tris–HCl buffer (pH 7.4), 50 µM NADPH, 10 µl DMSO or the same volume of DMSO solution containing the test compounds to a final concentration of 10^{-11}–10^{-5} M, and 10 µl of bovine liver dihydrofolate reductase (DHFR), in a final volume of 1.0 ml [61]. After addition of the enzyme, the mixture was incubated at room temperature for 2.0 min, and the reaction was started by adding 5 µl of dihydrofolic acid, the difference in absorbance (ΔOD/min) was measured by the spectrophotometer at 340 nm and 22 °C, kinetic program (reading repeated every 15 s for 2.5 min). Results are reported as % inhibition of enzymatic activity (Table 1) calculated by using the following equation:

$$\text{Fractional activity of enzyme} = (\text{Sample } \Delta\text{OD/min} - \text{blank } \Delta\text{OD/min}) \times d/12.3 \times V \times \text{mgP/ml}$$

where

ΔOD/min: the spectrophotometer readings.
12.3: extinction coefficient for the DHFR reaction at 340 nm.
V: Enzyme volume used in the assay in ml.
d: the enzyme sample dilution factor.
mgP/ml: the original sample enzyme concentration before dilution.

6.3. Molecular modeling study

The molecular modeling calculations were done using “molecular operating environment (MOE) version 2009.11” Chemical Computing Group Inc. software. The most stable conformer of newly synthesized ‘global-minima’ analogs was docked into the binding pocket of dihydrofolate reductase enzyme-binding domain which is in tertiary complex with dihydro-nicotinamide-adenine-dinucleotide phosphate (NADPH) and methotrexate (MTX), code ID 1DLS. It was obtained from the research collaboratory for structural bioinformatics Protein Data Bank. The hydrogens were added, then enzyme structure subjected to a refinement protocol by addition of the missed bonds and protein potential fixation where the constraints on the enzyme were gradually removed and minimized until the RMSD gradient was 0.01 kcal/mol Å. The

active site of the enzyme was detected using a radius of 10.0 Å around MTX. The three-dimensional structures of some selected substituted quinazoline derivatives, which represent most and least active dihydrofolate reductase inhibitors, in their neutral forms, were built using the builder interface of the MOE software. Conformational analysis of the selected compounds was performed using MMFF94 force field with root mean square (RMS) gradient of 0.01 kcal/mol Å. The flexible alignment of selected compounds were done using the flexible alignment tool of the program adjusting the energy cut off to 15 kcal/mol, and RMSD tolerance to 0.5. Molecular surfaces were obtained from the surfaces and maps tool of the MOE program. In the molecular surface maps, the pink colored regions have potential hydrogen bonding ability, blue regions are mild polar, and green ones are the hydrophobic regions [45,62].

References

[1] V. Bavetsias, J.H. Marriott, C. Melin, R. Kimbell, Z.S. Matusia, F.T. Boyle, A.L. Jackman, J. Med. Chem. 43 (2000) 1910–1926.
[2] J.B. Smaill, G.W. Rewcastle, J.A. Loo, K.D. Gries, O.H. Chan, E.L. Reyner, E. Lipka, H.D. Showalter, P.W. Vincent, W.L. Elliot, W.A. Denny, J. Med. Chem. 43 (2000) 1380–1397.
[3] A. Wissner, D.M. Berger, D.H. Boschelli, M.B. Floyd, L.M. Greenbertger, H. Tsou, E. Upeslacis, Y.F. Wang, N. Zhang, J. Med. Chem. 43 (2000) 3244–3256.
[4] H.J. Park, Y.S. Kim, J.S. Kim, E.J. Lee, Y.J. Yi, H.J. Hwang, M.E. Suh, C.K. Ryu, S.K. Lee, Bioorg. Med. Chem. Lett. 14 (2004) 3385–3388.
[5] Z. Ma, Y. Hano, T. Nomura, Y. Chen, Bioorg. Med. Chem. Lett. 14 (2004) 1193–1196.
[6] N. Malecki, P. Carato, B. Riao, J.F. Goosens, R. Houssin, C. Bailly, J.P. Henichart, Bioorg. Med. Chem. 12 (2004) 641–647.
[7] V.M. Sharma, P. Prasana, K.V. Adi Seshu, C.L.L. Rao, G.S. Kumar, C.P. Narasimhulu, P.A. Babu, R.C. Puranik, D. Subramanyam, A.V. Warlu, S. Rajagopal, K.B.S. Kumar, R. Ajaykumar, R. Rajagopalan, Bioorg. Med. Chem. Lett. 12 (2002) 2303–2307.
[8] A.M.F. Kersemaekers, G.J. Fleuren, E.G. Kenter, L.J. Van den Broek, S.M. Uljee, J. Hermans, M.J. Van de Vijver, Clin. Cancer Res. 5 (1999) 577–586.
[9] M. Maurizi, G. Almadori, G. Ferrandina, M. Distefano, M.E. Romanni, G. Cadoni, P. Benedetti-Panici, G. Paludetti, G. Scambia, S. Mancuso, Br. J. Cancer 74 (1996) 1253–1257.
[10] A.L. Harries, Int. J. Radiat. Biol. 48 (1985) 675–690.
[11] A.M. Thompson, A.J. Bridges, D.W. Fry, A.J. Kraker, W.A. Denny, J. Med. Chem. 38 (1995) 3780–3788.
[12] A.J. Bridges, H. Zhou, D.R. Cody, G.W. Rewcastle, A. McMichael, H.D. Showalter, D.W. Fry, A.J. Kraker, W.A. Denny, J. Med. Chem. 39 (1996) 267–276.
[13] A.E. Wakeling, A.J. Barker, D.H. Davies, D.S. Brown, L.R. Green, S.A. Cartlidge, J.R. Woodburn, Breast Cancer Res. Treat. 38 (1996) 67–73.
[14] R.J. Griffin, S. Srinivasan, K. Bowman, A.H. Calvert, N.J. Curtin, D.R. Newell, L.C. Pemberton, B.T. Golding, J. Med. Chem.. 41 (1998) 5247–5256.
[15] J. Jolivet, K.H. Cowan, G.A. Curt, N.J. Clendeninn, B.A. Chabner, N. Eng. J. Med. 309 (1983) 1094–1104.
[16] R.D. Wit, S. Kaye, J. Roberts, G. Stoter, J. Scott, J. Verweij, Br. J. Cancer. 67 (1993) 388–390.
[17] P.A. Nguewa, M.A. Fuertes, V. Cepeda, S. Iborra, J. Carrión, B. Valladares, et al., Chem. Biodiver. 2 (2005) 1387–1400.
[18] B.I. Schweitzer, A.P. Dicker, J.R. Bertino, FASEB J. 4 (1990) 2441–2452.
[19] A. Gangjee, J. Yu, J.J. Mcguire, V. Cody, N. Galitsky, R.L. Kisliuk, et al., J. Med. Chem. 43 (2000) 3837–3851.
[20] S.T. Al-Rashood, I.A. Aboldahab, M.N. Nagi, L.A. Abouzeid, A.A. Abdel-Aziz, S.G. Abdel-Hamide, et al., Bioorg. Med. Chem. 14 (2006) 8608–8621.
[21] Y.I. El-Gazzar, H.H. Georgey, S.M. El-Messery, H.A. Ewida, G.S. Hassan, M.M. Raafat, et al., Bioorg. Chem. 72 (2017) 282–292.
[22] H.I. El-Subbagh, M.A. El-Sherbeny, M.N. Nasr, F.E. Goda, F.A. Badria, Boll. Chim. Farm. 134 (1995) 80–84.
[23] H.I. El-Subbagh, A.M. Al-Obaid, Eur. J. Med. Chem. 31 (1996) 1017–1021.
[24] H.I. El-Subbagh, W.A. El-Naggar, F.A. Badria, Med. Chem. Res. 3 (1994) 503–516.
[25] E. Schützneverová, I. Popa, V. Kryštof, H. Koshino, Z. Trávníček, P. Hradil, et al., Tetrahedron 68 (2012) 3996–4002.
[26] H. Kaur, S.M. Lim, K. Ramasamy, M. Vasudevan, S.A.A. Shah, B. Narasimhan, Arab. J. Chem. (2017).
[27] X. Li, M. Hilgers, M. Cunningham, Z. Chen, M. Trzoss, J. Zhang, L. Kohnen, T. Lam, C. Creighton, K. Gc, K. Nelson, B. Kwan, M. Stidham, V. Brown-Driver, K.J. Shaw, J. Finn. Bioorg. Med. Chem. Lett. 21 (2011) 5171–5176.
[28] A. Aouidate, A. Ghaleb, M. Ghamali, S. Chtita, M. Choukrad, A. Sbai, et al., J. Mol. Struct. 1139 (2017) 319–327.
[29] F.A. Al-Omary, G.S. Hassan, S.M. El-Messery, M.N. Nagi, E.-S.E. Habib, H.I. El-Subbagh, Eur. J. Med. Chem. 63 (2013) 33–45.
[30] S.T. Al-Rashood, G.S. Hassan, S.M. El-Messery, M.N. Nagi, E.-S.E. Habib, F.A. Al-Omary, et al., Bioorg. Med. Chem. Lett. 24 (2014) 4557–4567.
[31] A.S. El-Azab, A.A.-M. Abdel-Aziz, H.A. Ghabbour, M.A. Al-Gendy, J. Enz. Inhib. Med. Chem. 32 (2017) 1229–1239.
[32] T. Mosmann, J. Immunol. Methods. 65 (1983) 55–63.
[33] F. Denizot, R. Lang, J. Immunol. Methods. 89 (1986) 271–277.
[34] M. Metwally, M. Gouda, A.N. Harmal, A. Khalil, Eur. J. Med. Chem. 56 (2012) 254–262.
[35] B. Liu, M. Fang, M. Schmidt, Y. Lu, J. Mendelsohn, Z. Fan, Br. J. Cancer 82 (2000) 1991–1999.
[36] D. Bernhard, W. Schwaiger, R. Crazzolara, I. Tinhofer, R. Kofler, A. Csordas, Cancer Lett. 195 (2003) 193–199.
[37] M. Pagliacci, F. Spinozzi, G. Migliorati, G. Fumi, M. Smacchia, F. Grignani, et al., Eur. J. Cancer 29 (1993) 1573–1577.
[38] M.G. Ormerod, J. Immunol. Methods. 265 (2002) 73–80.
[39] L.C. Falk, D.R. Clark, S.M. Kalman, T.F. Long, Clin. Chem. 22 (1976) 785–788.
[40] D.L. Peterson, J.M. Gleisner, R.L. Blakley, Biochem. 14 (1975) 5261–5267.
[41] H.I. El-Subbagh, A.H. Abadi, H.A. Al-Khamees, Arch. Pharm. (Weinheim). 330 (1997) 277–284.
[42] A. Saxena, D. Wong, K. Diraviyam, D. Sept, Methods Enzymol. (2009) 307–334.
[43] L. Ferreira, R.D. Santos, G. Oliva, A. Andricopulo, Molec. 20 (2015) 13384–13421.
[44] T.A. Halgren, J. Comput. Chem. 17 (1996) 520–552.
[45] MOE 2009.10 of Chemical Computing Group. Inc. https://www.chemcomp.com/.
[46] W.S. Lewis, V. Cody, N. Galitsky, J.R. Luft, W. Pangborn, S.K. Chunduru, et al., J. Biol. Chem. 270 (1995) 5057–5064.
[47] M. Graffner-Nordberg, K. Kolmodin, J. Åqvist, S.F. Queener, A. Hallberg, J. Med. Chem. 44 (2001) 2391–2402.
[48] P. Labute, C. Williams, M. Feher, E. Sourial, J.M. Schmidt, J. Med. Chem. 44 (2001) 1483–1490.
[49] M.D. Miller, R.P. Sheridan, S.K. Kearsley, J. Med. Chem. 42 (1999) 1505–1514.
[50] S.K. Kearsley, G.M. Smith, Tetrahed. Comp. Methodol. 3 (1990) 615–633.
[51] K.W. Lexa, H.A. Carlson, Quarterly Rev. Biophy. 45 (2012) 301–343.
[52] C.A. Lipinski, Drug Disc. Today: Technol. 1 (2004) 337–341.
[53] D.E. Clark, S.D. Pickett, Drug Disc. Today 5 (2000) 49–58.
[54] W.P. Walters, Expert Opin. Drug Disc. 7 (2012) 99–107.
[55] T. Lynch, A. Price, Am. Fam. Physician 76 (2007) 391–396.
[56] M.T.H. Khan, Curr. Drug Metab. 11 (2010) 285–295.
[57] F. Cheng, W. Li, Y. Zhou, J. Shen, Z. Wu, G. Liu, et al., J. Chem. Inform. Model. 52 (2012) 3099–3105.
[58] Y. Li, Y. Tyan, H. Kuo, W. Chang, T. Hsia, J. Chung, Food Chem.Toxicol. 42 (2004) 37–43.
[59] E. Lee, Y.-J. Surh, Cancer Lett. 134 (1998) 163–168.
[60] K.K.-W. Lo, T.K.-M. Lee, J.S.-Y. Lau, W.-L. Poon, S.-H. Cheng, Inorg. Chem. 47 (2008) 200–208.
[61] R. Pignatello, G. Spampinato, V. Sorrenti, L. Vicari, C.D. Giacomo, A. Vanella, et al., Pharm. Pharmacol. Commun. 5 (1999) 299–305.
[62] T.A. Halgren, J. Comput. Chem. 17 (1996) 490–519.